Landsvirkjun

LV-2023-060

Seismic Monitoring in Krafla, Þeistareykir and Námafjall

October 2022 to November 2023

Seismic Monitoring in Krafla, Þeistareykir and Námafjall

October 2022 to November 2023

Egill Árni Guðnason, Þorbjörg Ágústsdóttir,
Rögnvaldur Líndal Magnússon and Karl Gunnarsson

December 2023

ÍSOR-2023/043
Project no.: 23-0077

Key Page

Report LV no.	LV-2023-060	**Date**	December 2023
Number of pages	40	**Copies**	1
Distribution	[X] On www.lv.is	[X] Open	[ ] Limited until [date]
Title	Seismic Monitoring in Krafla, Þeistareykir and Námafjall. Reprocessing of the Entire 2006–2022 Catalogue		
Authors/Company	Egill Árni Guðnason, Þorbjörg Ágústsdóttir, Rögnvaldur Líndal Magnússon and Karl Gunnarsson		
Project managers	Anette K. Mortensen (LV) and Egill Árni Guðnason (ÍSOR)		
Prepared for	Prepared by Iceland GeoSurvey (ÍSOR) for Landsvirkjun (LV)		
Co-operators	—		

Abstract

The annual results of earthquake monitoring in the geothermal areas of Krafla, Þeistareykir and Námafjall for the period from 1st of October 2022 to the 31st of October 2023 are reported. Around 5,300 earthquakes were located, with the highest concentration of earthquakes in Krafla, and lowest in Námafjall. Micro-seismicity is dominant in all areas, with only three events exceeding magnitude M_L 2.0.

The observed seismicity rate in Krafla and Námafjall is similar to last year, while there is a significant increase in Þeistareykir. The increase within the Tjarnarás cluster coincides with the start of an ongoing inflation in Þeistareykir. Drilling and stimulation of two new wells in Þeistareykir in 2023 did not induce any significant earthquake activity.

Double-couple focal mechanisms are calculated for a total of 343 earthquakes. Diverse faulting styles are inferred, with normal faulting dominant in Krafla, while the stress regime is very different in both Þeistareykir and Námafjall, where strike-slip faulting is dominant. 35 earthquakes in Krafla are attributed to non-double-couple mechanisms, both explosive and implosive.

From 2021 to 2023, the Vp/Vs ratio in Krafla increases slightly, compared to previous years, while the ratios in Þeistareykir and Námafjall are a little higher and more variable.

Keywords Krafla, Þeistareykir, Námafjall, earthquakes, seismicity, monitoring, production, re-injection, brittle-ductile, focal mechanism, double-couple, Landsvirkjun, ÍSOR

Project manager's signature	Reviewed by
Egill Árni Guðnason	Arnar Már Vilhjálmsson

Approved by Landsvirkjun's project manager

Anette K. Mortensen

Table of contents

1 Introduction **7**

2 The seismic network **7**

3 Seismic characteristics **7**

3.1 Krafla 10
3.2 Þeistareykir 13
3.3 Námafjall 17

4 Focal mechanisms **19**

4.1 Krafla 21
4.2 Þeistareykir 23
4.3 Námafjall 25
4.4 Non-double-couple earthquakes 27

5 Vp/Vs ratio **29**

6 Conclusions **32**

References **34**

Appendix A: Seismicity in Þeistareykir **37**

Appendix B: Non-double-couple earthquakes in Krafla **39**

Appendix C: Vp/Vs ratio for 2021-2022 ..... **40**

List of tables

Table 1. *Calculated Vp/Vs ratio for Krafla, Þeistareykir and Námafjall 2016-2017 to 2022-2023* 32

List of figures

Figure 1. *Refined manual earthquake locations of 5,275 earthquakes in the Krafla, Þeistareykir and Námafjall geothermal areas during the study period, in map and depth view* 9

Figure 2. *Refined manual earthquake locations of 3,672 earthquakes in the Krafla geothermal area during the study period, in map and depth view* 11

Figure 3. *Time vs. magnitude (M_L) plot of the 3,672 located earthquakes in the Krafla geothermal area during the study period* 12

Figure 4. *Time vs. depth and latitude of located earthquakes in the Krafla geothermal area during the study period* 12

Figure 5. *Refined manual earthquake locations of 1,471 earthquakes in the Þeistareykir geothermal area during the study period, in map and depth view* 15

Figure 6. *Time vs. magnitude (M_L) plot of the 1,471 located earthquakes in the Þeistareykir geothermal area during the study period* 16

Figure 7. *Time vs. depth and latitude of located earthquakes in the Þeistareykir geothermal area during the study period. Earthquakes are colour-coded by depth.* 17

Figure 8. *Refined manual earthquake locations of 100 earthquakes in the Námafjall geothermal area during the study period, in map and depth view* 18
Figure 9. *Time vs. magnitude (M_L) plot of the 100 located earthquakes in the Námafjall geothermal area during the study period* 19
Figure 10. *Graphic summary of all 343 double-couple focal mechanisms located in Krafla, Þeistareykir and Námafjall geothermal areas during the study period* 20
Figure 11. *A Frohlich mechanism categorisation plot for all 343 double-couple focal mechanisms displayed in Figure 10* 21
Figure 12. *Map view of double-couple focal mechanisms for 216 selected events in the Krafla geothermal area during the study period* 22
Figure 13. *A Frohlich focal mechanism categorisation plot for the 216 double-couple focal mechanisms in Krafla, displayed in map view in Figure 12* 23
Figure 14. *Map view of double-couple focal mechanisms for 115 selected events in the Þeistareykir geothermal area during the study period* 24
Figure 15. *A Frohlich focal mechanism categorisation plot for the 115 double-couple focal mechanisms in Þeistareykir, displayed in map view in Figure 14* 25
Figure 16. *Map view of double-couple focal mechanisms for 12 selected events in the Námafjall geothermal area during the study period* 26
Figure 17. *A Frohlich focal mechanism categorisation plot for the 12 double-couple focal mechanisms in Námafjall, displayed in map view in Figure 16* 27
Figure 18. *Pure non-double-couple earthquakes in the Krafla geothermal area during the study period, in map and depth view* 28
Figure 19. *Calculated Vp/Vs ratio for the Krafla, Þeistareykir and Námafjall geothermal areas during the study period, from top to bottom, respectively.* 31

1 Introduction

Seismic activity is monitored in the three developed high-temperature geothermal areas of the Northern Volcanic Zone, NE Iceland; Krafla, Þeistareykir and Námafjall. The local seismic network is operated by Iceland GeoSurvey (ÍSOR) on behalf of the National Power Company of Iceland, Landsvirkjun (LV), and consists of 21 stations in total, supplemented with 6 stations from the regional seismic network of the Icelandic Meteorological Office (IMO) (Figure 1).

The purpose of the dense seismic network is to monitor seismic activity associated with the utilisation of the three respective geothermal systems, as well as to monitor natural activity in these volcanic environments. The raw seismic data are automatically streamed to ÍSOR, where they are processed in real-time. All detected earthquakes are manually reviewed and refined. The operation of the seismic network since 2006 has provided a large and interesting dataset of earthquakes, and results have been published in both yearly reports by ÍSOR (e.g., Guðnason et al., 2022 and references therein) and in an overview report, where the entire catalogue (2006-2022) was reprocessed (Guðnason et al., 2023).

This annual report presents results of earthquake monitoring in the geothermal areas of Krafla, Þeistareykir and Námafjall, for the period from the 1st of October 2022 to the 31st of October 2023. In line with the project contract, the report contains e.g., refined earthquake locations, focal mechanisms of selected earthquakes and a calculation of the Vp/Vs ratio for all three areas.

2 The seismic network

The LV/ÍSOR seismic network consists of 21 permanent stations (Figure 1). The geometry of the seismic network in the Krafla and Námafjall areas has remained the same since 2015 and 2017, respectively, while the seismic network in Þeistareykir was expanded in 2021, with three stations from the German Research Centre for Geosciences (GFZ) added to the permanent LV/ÍSOR seismic network.

3 Seismic characteristics

From the 1st of October 2022 to the 31st of October 2023, a total of 5,275 earthquakes were detected and located in the Krafla, Þeistareykir and Námafjall geothermal areas, and surroundings (Figure 1). For comparison, the regional seismic network of the Icelandic Meteorological Office (IMO) in Iceland located 572 earthquakes in the same area during this period, or ~11%.

Rate

It should be noted that the time period covered in this report is extended to 13 months, instead of 12 months or less in the most recent yearly reports by ÍSOR. There are only small variations in the observed seismicity rate in the Krafla and Námafjall areas, compared to last year (Guðnason et al., 2022), while there is a significant increase in Þeistareykir, further discussed in chapter 3.2. However, as before, the number of earthquakes in Krafla is higher compared to Þeistareykir and Námafjall. In total, 3,672 earthquakes were located in the Krafla geothermal area (282/month on average, compared to 255/month last year), 1,471 earthquakes in the

Þeistareykir geothermal area (113/month on average, compared to 55/month last year) and 100 earthquakes in the Námafjall geothermal area (8/month on average, compared to 11/month last year). A small number of events are located along the volcanic rift zone north of Krafla and southeast of Þeistareykir, which are outside the scope of this report.

Processing

All earthquakes were automatically detected and located in real-time using the SeisComP software (https://www.seiscomp.de/), and all were manually reviewed and refined. For the purpose of this report, all earthquake locations were refined using the NonLinLoc algorithm (Lomax et al., 2000) in order to improve the earthquake location, which takes the absolute elevation of the seismic stations into account in the location routine. All earthquakes are located using a gradient version of the ÍSOR velocity model, based on processing and interpretation of refraction surveys performed in Krafla in 1961-1963 and 1971-1973 (Ágústsson et al., 2011), except earthquakes in the Þeistareykir area, which are located using a gradient local velocity model for the area (Guðnason and Ágústsdóttir, 2021).

Magnitudes

All recorded earthquakes are small, with 99% of M_L < 1.0. Three events exceed M_L 2.0 (Figure 1); one originating relatively deep within the Krafla fissure swarm (Figure 2), and two originating in Þeistareykir, within the Randir/Hitur and Tjarnarás clusters (Figure 5). As before, seasonal fluctuations are observed in the magnitude range in all three geothermal areas (Figures 3, 6 and 9), whereas this signal is strongest in Krafla. The daily seismicity rate in Krafla is greatest during the winter months throughout May, similarly in Námafjall, while in Þeistareykir, there is an observed increase in seismicity rate several times throughout the winter and spring, further discussed in chapter 3.2. The sensitivity of the seismic network in all areas is higher during the summer months, with smaller magnitude events detected, most likely due to better weather conditions.

Brittle-ductile transition

The brittle-ductile transition in the three geothermal areas is rather variable from one area to the other (Figure 1). In particular, it domes up to shallowest depths below the Krafla well field, but also below Mt. Bæjarfjall in Þeistareykir and to some extent below the Námafjall well field. In the following chapters, 3.1-3.3, results are presented for individual geothermal areas separately.

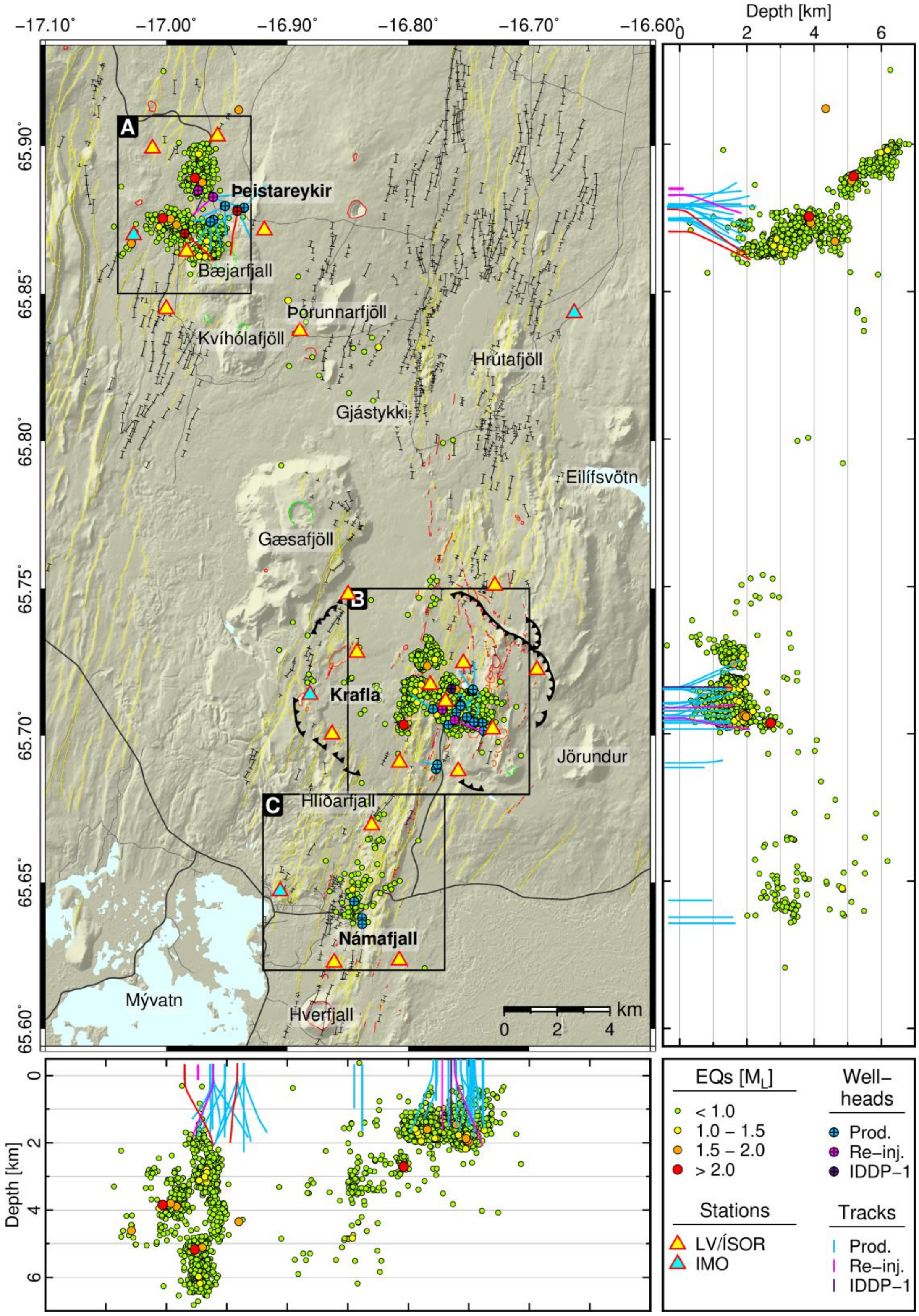

Figure 1. *Refined manual earthquake locations of 5,275 earthquakes in the Krafla, Þeistareykir and Námafjall geothermal areas during the study period, in map and depth view. Earthquake locations are colour-coded according to magnitude. See legend for different seismic stations, wellheads and well trajectories. Mapped geological structures are from Sæmundsson et al. (2012). Main roads are in black, and main landmarks referenced in the text are shown on the map. Black boxes mark the outlines of the zoomed-in view of each geothermal area as shown in Figures 2, 5 and 8.*

3.1 Krafla

Earthquake activity in the Krafla geothermal area is shallow, with 95% of located earthquakes confined to the depth range of 1-2 km below sea level (Figure 2). As before, the activity occurs in at least four spatially divided clusters (Schuler et al., 2015a), which are separated by areas of little or no seismicity.

Three of the four clusters originate within the fissure swarm transecting Leirhnjúkur, with seismicity within the cluster furthest to the SSW slightly deeper than elsewhere in Krafla, within a confined depth range of around 2.5-3 km. Earthquake activity within the fissure swarm is around 20% of the total number of earthquakes in the Krafla area during the study period (Figure 3), and is most likely a combination of i) circulating geothermal fluids and ii) dyke contraction from the Krafla rifting episode in 1975-1989 (Einarsson, 1991).

The fourth and largest cluster in the Leirbotnar-Suðurhlíðar area is the most seismically active and confined to the Krafla geothermal well field, with around 80% of located earthquakes in the area (Figure 3). The micro-seismic activity in this area is more or less constant between 1-2 km depth, with the highest seismicity rate during the winter months, and a higher daily rate of earthquakes in between, but no specific earthquake swarms are observed during the past year.

Magnitudes

Magnitudes in Krafla during the study period range from M_L -0.5 to 2.1 (Figure 3). Earthquakes of $M_L > 1$ are within 1% of the total catalogue in Krafla, and the majority of these "larger" earthquakes are confined to the deeper end of the depth range, with the largest earthquake occurring within the deepest cluster (Figure 2). This indicates that the crust in Krafla is strongest, or under most strain, close to the shallow brittle-ductile transition. Seasonal fluctuations are observed in the magnitude distribution, with smaller earthquakes detected during summer, than during winter.

Spatial and temporal distribution

The depth distribution of earthquakes in Krafla suggests that the brittle-ductile transition is at around 2 km depth, where temperatures of 600-700°C are expected in basaltic rocks (Ágústsson and Flóvenz, 2005; Violay et al., 2012; Bali et al., 2020; Flóvenz et al., 2020). This is partly confirmed by the two geothermal wells that encountered magma during drilling, i.e., wells KJ-39 (Árnadóttir et al., 2009) and IDDP-1 (Mortensen et al., 2014). Both wells are drilled down to the brittle-ductile transition at 2 km depth (Figure 2), close to the upper boundary of a low Vp/Vs anomaly observed below the well field (Schuler et al., 2015a) and large amplitude reflections ("bright spots") mapped beneath well IDDP-1 using reflection imaging of micro-earthquakes, corresponding to magma (Kim et al., 2020).

Looking at the micro-seismic activity in Krafla as i) depth and ii) longitude as a function of time, it is evident that the activity is in general rather constant, in particular within the well field, but also within the fissure swarm. A gap in seismicity in December 2022 is related to extreme winter conditions in Krafla causing power loss at many seismic stations, and a subsequently low seismic sensitivity in the area (Figures 3 and 4). Due to a local weaker crust in Krafla (high *b*-value), stress is released early by numerous, small earthquakes, and thus, earthquake swarms or large magnitude earthquakes are rarely observed (Guðnason et al., 2021).

Rate

In Krafla, small-amplitude aftershocks are occasionally observed in the seismic waveform of larger-amplitude earthquakes, but more frequently, earthquakes with similar waveforms and magnitudes, separated only by a few seconds are observed (Guðnason et al., 2021), referred to as multiplets by Schuler et al. (2016). During the study period, these multiplets are again observed, while days of higher seismicity rate rarely occur all in one swarm on a single fault, or in a confined area.

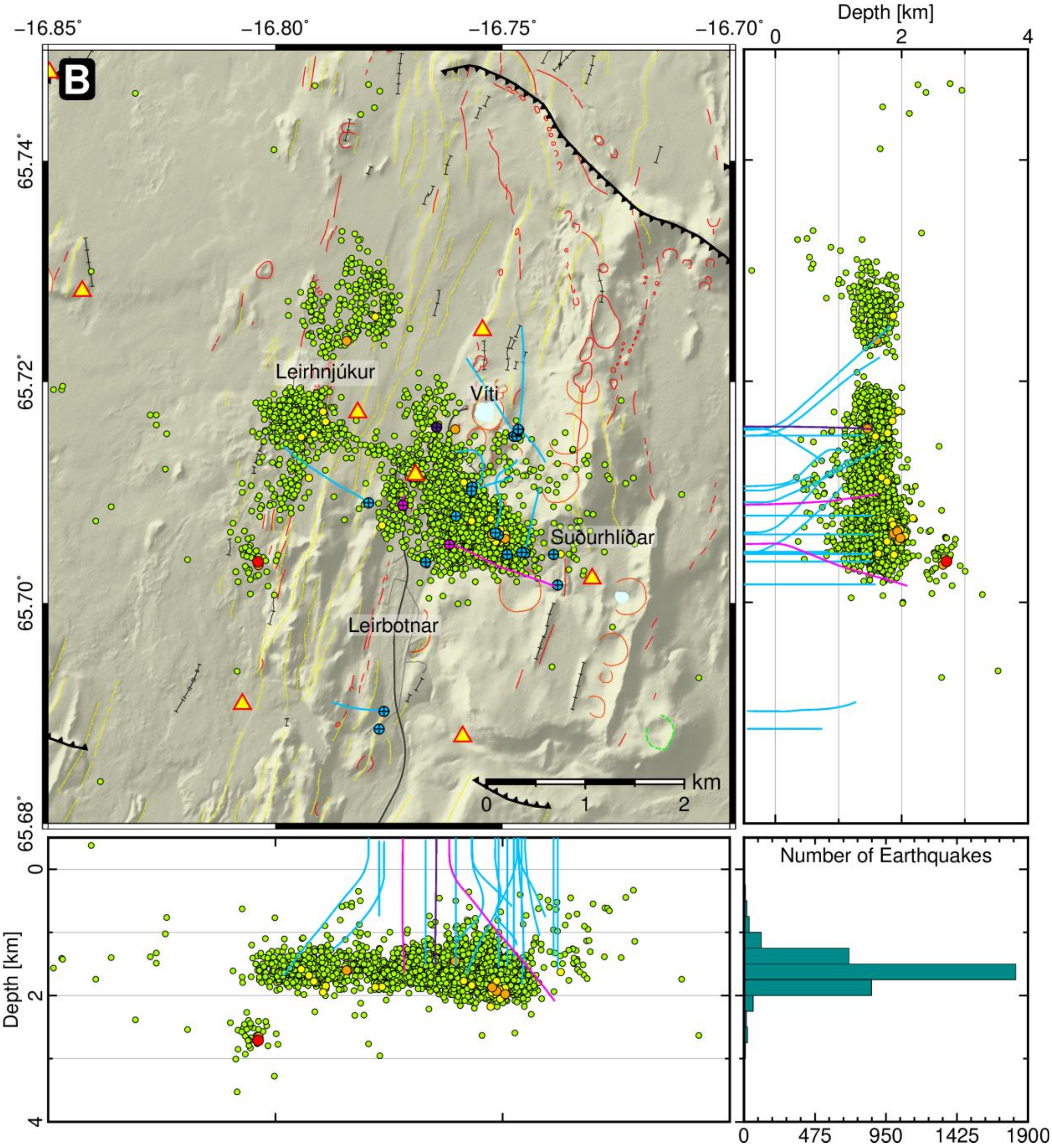

Figure 2. *Refined manual earthquake locations of 3,672 earthquakes in the Krafla geothermal area (box B in Figure 1) during the study period, in map and depth view. See legend and figure caption from Figure 1 for references to the map.*

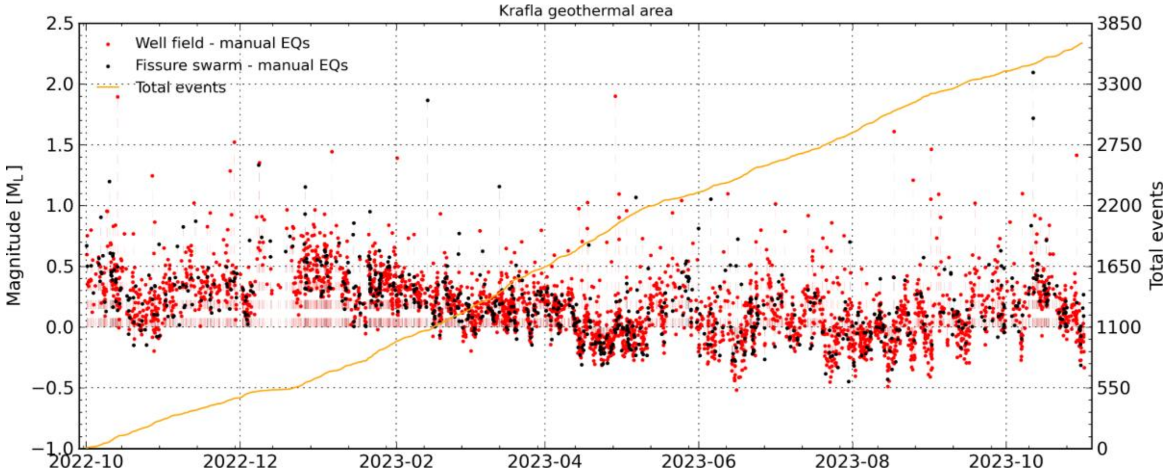

Figure 3. *Time vs. magnitude (M_L) plot of the 3,672 located earthquakes in the Krafla geothermal area (box B in Figure 1) during the study period. Manual earthquakes are shown as different coloured dots, referring to the two different clusters of the well field (red) and the fissure swarm (black). The orange line shows the cumulative number of earthquakes.*

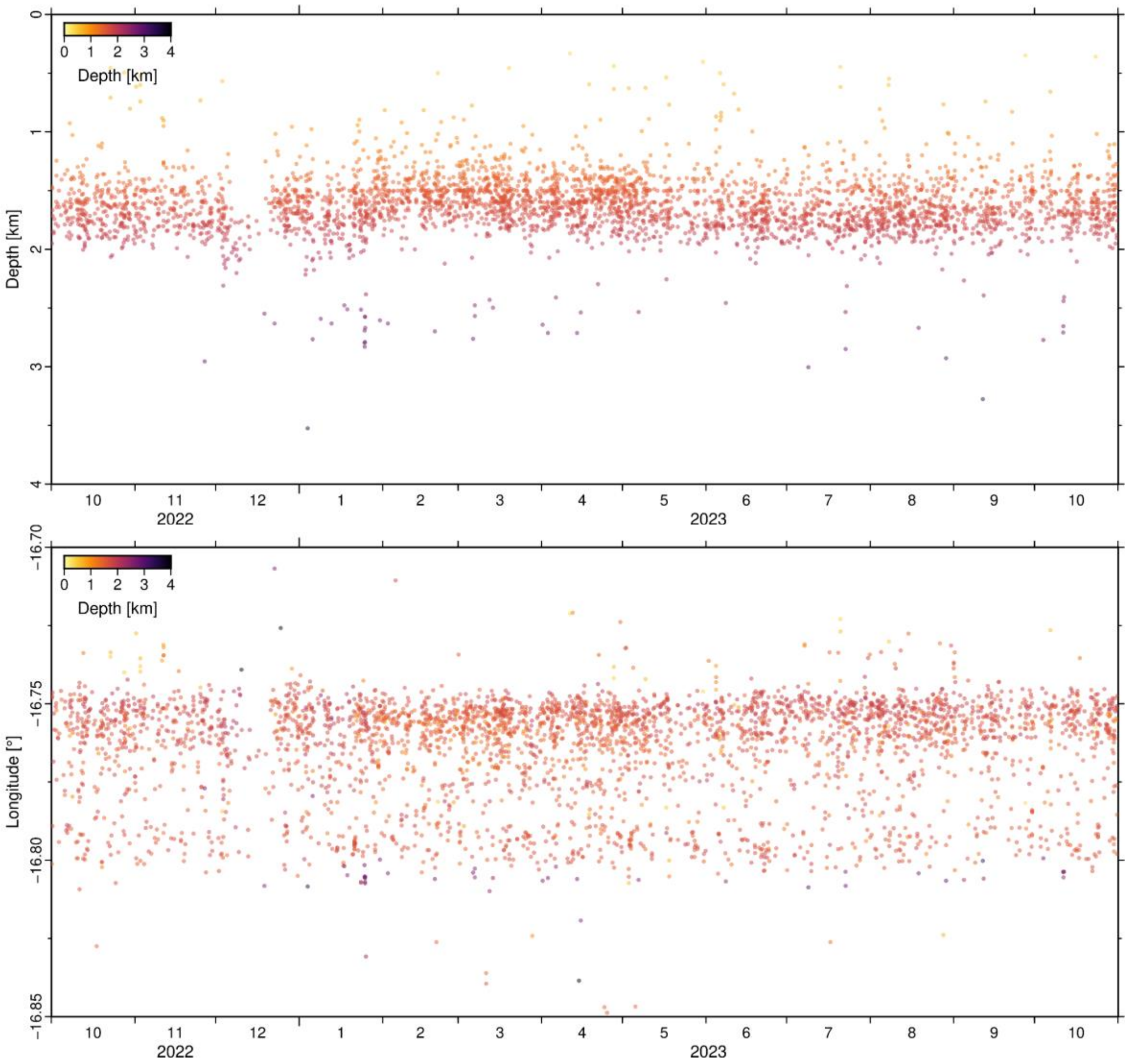

Figure 4. *Time vs. depth (top) and latitude (bottom) of located earthquakes in the Krafla geothermal area (box B in Figure 1) during the study period. Earthquakes are colour-coded by depth.*

3.2 Þeistareykir

Earthquake activity in the Þeistareykir geothermal area occurs, as before, in more or less three spatially separated clusters during the study period (Figures 5 and A1 in Appendix A). The majority of earthquakes are confined to the well-defined cluster below the northwest flanks of Mt. Bæjarfjall, within the depth range of 2-3.5 km, which most likely represents an up-doming of the brittle-ductile transition in Þeistareykir, where high temperatures are expected, as discussed in e.g., Guðnason et al. (2023). The other two clusters in Randir/Hitur and in Tjarnarás are smaller and confined to greater depths, > 3.5 km (Figures 5 and A1 in Appendix A). However, there is an observed increase in earthquake activity within both clusters during the study period, further discussed below (Figures 6 and A2 in Appendix A). A tiny cluster of earthquakes is observed at 1.5-2 km depth just northwest of Mt. Bæjarfjall, where geothermal manifestations are observed on the surface.

Drilling

Drilling of two new wells in Þeistareykir, i.e., wells ÞG-19 and ÞG-20, was completed in 2023 (Figures 5 and A1 in Appendix A). Both wells are directionally drilled below Mt. Bæjarfjall; well ÞG-19 from the northwest side of Mt. Bæjarfjall to its crater at a final depth of 3,000 m and well ÞG-20 from the north side of Mt. Bæjarfjall to its crater at final depth of 3,000 m (Jóngeirsdóttir et al., 2023a, 2023b). The aim of wells ÞG-19 and ÞG-20 was to confirm and test mapped fault systems on the western side of Mt. Bæjarfjall, and below the NNE flank of Mt. Bæjarfjall and into the crater rim fault (Blischke et al., 2023). The wells were drilled from June to October 2023, or more precisely, well ÞG-19 from the 3rd of June to the 6th of August, and well ÞG-20 from the 26th of August to the 14th of October. The drilling and the subsequent stimulation of the two wells does not seem to have induced any significant earthquake activity below Mt. Bæjarfjall, further confirming the theory that the Mt. Bæjarfjall cluster is of natural origin, most likely representing the up-flow zone of the Þeistareykir geothermal system (Figures 7 and A2 in Appendix A) (e.g., Guðnason et al., 2023).

Magnitudes

Magnitudes in Þeistareykir during the study period range from M_L -1 to 2.4 (Figure 6 and A2 in Appendix A). Earthquakes of M_L > 1.0 are few, around 1% of the total catalogue in Þeistareykir. The two largest earthquakes of M_L 2.2 and 2.4 occur within the Tjarnarás and Randir/Hitur clusters, respectively. The majority of these "larger" earthquakes are confined to the deeper end of the depth range, indicating that the crust in Þeistareykir is strongest, or under most strain, close to the varying brittle-ductile transition in the area. Some of the larger events during the study period have been felt at the Þeistareykir power plant (Anette K. Mortensen, personal communication, September 2023). As in Krafla, seasonal fluctuations are observed in the magnitude distribution, with smaller earthquakes detected during summer, than during winter.

Spatial and temporal distribution

Looking at the micro-seismic activity in Þeistareykir as i) depth and ii) latitude as a function of time, it is evident that the activity within the Mt. Bæjarfjall cluster is in general rather constant, confirming that drilling of the two new wells in 2023 did not induce any significant activity (Figure 7). The activity within the Randir/Hitur and Tjarnarás clusters is more scattered in time, although there is an observed increase in activity within both clusters, further discussed below.

In general, the depth distribution of seismicity in Þeistareykir (since late 2014) suggests that the brittle-ductile transition is shallowest at ~3.5 km depth below the northwest flanks of Mt. Bæjarfjall, coinciding with a part of the main production field, where temperatures of 600-700°C are expected (Figure 5) (Guðnason et al., 2023). Immediately north of Mt. Bæjarfjall, within the Randir/Hitur cluster, the brittle-ductile transition is located at ~4 km depth, deepening further within the fissure swarm towards north to 5.5-7 km depth. Earthquake activity in Þeistareykir, however, is shallowest (~2 km) within the tiny cluster of earthquakes just northwest of Mt. Bæjarfjall.

Rate

Seismicity in Þeistareykir is thought to be mainly of natural origin, as discussed in e.g., Guðnason et al. (2023) and Schuler et al. (2015b), as it has prevailed in more or less the same three spatially separated clusters since years before utilisation of the geothermal field started in 2017. Last year, an observed increase in seismicity rate in Þeistareykir was attributed to the increased seismic sensitivity in the area since late July 2021, when three new stations were added to the permanent LV/ÍSOR seismic network (Guðnason et al., 2022).

During the study period, however, there is an overall observed increase in seismicity rate in the area, which originates within both the Randir/Hitur and the Tjarnarás cluster (Figures 6, 7 and A2 in Appendix A). The increase within the Randir/Hitur cluster occurred mainly during two earthquake swarms, in early November (1st to 6th) and the middle of December (10th to 17th) 2022, with a few earthquakes exceeding M_L 1.5, and the largest one of M_L 2.4 on the 12th of December (Guðnason and Ágústsdóttir, 2023). The depth of these earthquakes is between ~3 and 4.5 km, similar to what has previously been observed. This increased activity is most likely of purely natural origin. Since the two swarms occurred, the seismicity rate within the Randir/Hitur cluster has been relatively constant, with a slight increase in June 2023 (Figures 6, 7 and A2 in Appendix A).

The observed increase in seismicity rate within the Tjarnarás cluster started in late February – early March 2023, coinciding with the start of an inflation in Þeistareykir (Figures 6, 7 and A2 in Appendix A) (Drouin, 2023). The centre of uplift is approximately 2.5 km west of the Þeistareykir power plant, and at the time of writing, the maximum uplift has reached ~3 cm. The seismic activity within the Tjarnarás cluster peaked during an earthquake swarm from the 10th to the 12th of April, with a maximum magnitude earthquake of M_L 1.4 occurring at 6.2 km depth. Since then, the seismicity rate within the cluster has been relatively constant, with a slight increase in June 2023, and again in late September – early October, when the largest earthquake of M_L 2.2 occurred at 5.2 km depth. The depth of the earthquakes within the Tjarnarás cluster is between ~4.8 to 6.8 km, deepening towards north, similar to what has previously been observed. Earthquake depths also coincide with the modelled volume increase causing the inflation at ~4.5-6 km depth (Drouin, 2023). Thus it is concluded that the increased activity within the Tjarnarás cluster is of natural origin, and most likely a crustal response to the observed and ongoing inflation in the area.

In general, the high *b*-value calculated in Þeistareykir the last few years indicates a local weaker crust in which stress cannot build up to very high levels (Guðnason et al., 2021). Instead, stress is released early by numerous, small earthquakes. However, occasional small, short-lived earthquake swarms do occur in Þeistareykir, different to Krafla (Figures 6, 7 and A2 in Appendix A).

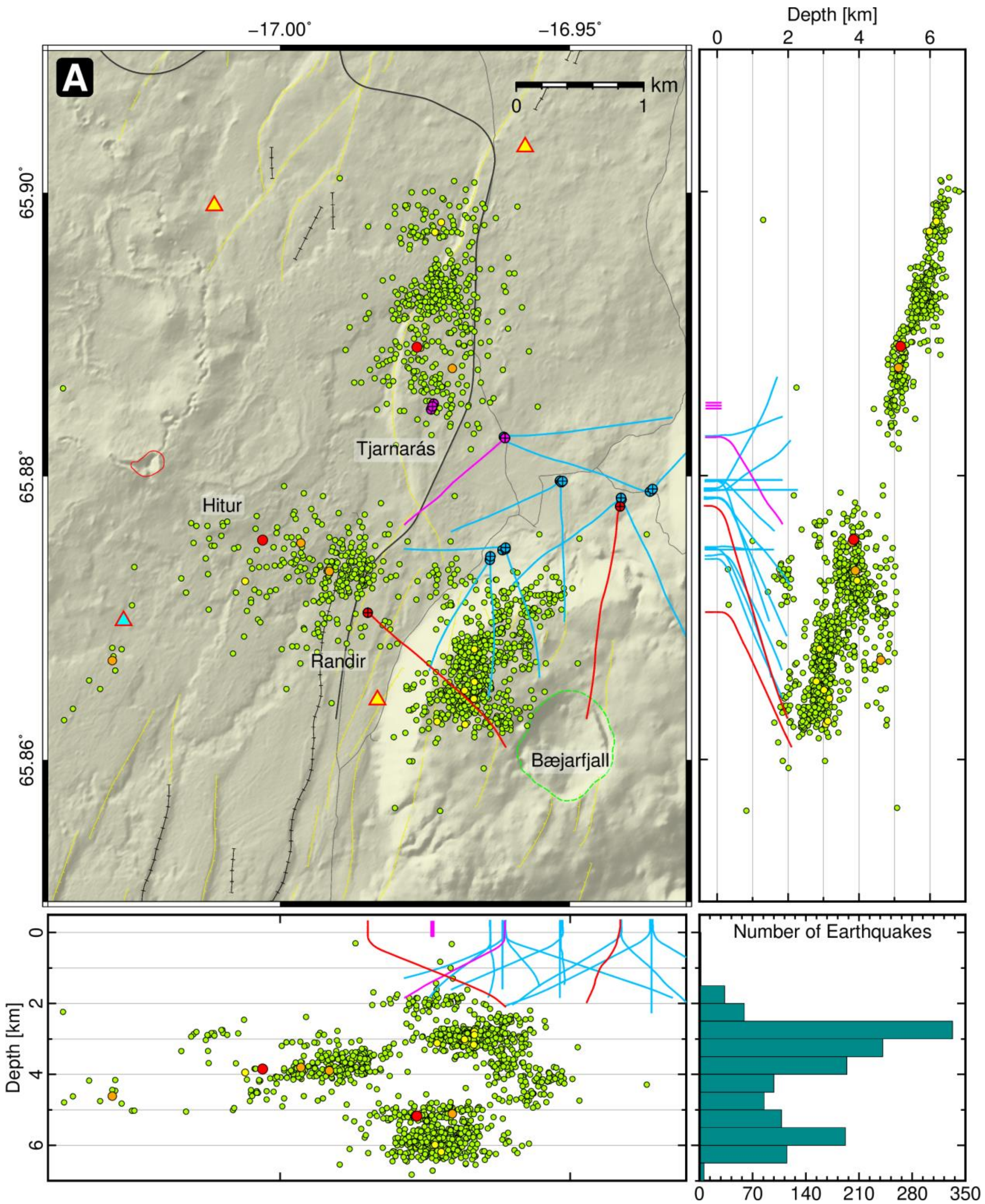

Figure 5. *Refined manual earthquake locations of 1,471 earthquakes in the Þeistareykir geothermal area (box A in Figure 1) during the study period, in map and depth view. See legend and figure caption from Figure 1 for references to the map. The two new wells, ÞG-19 and ÞG-20, are highlighted in red colour.*

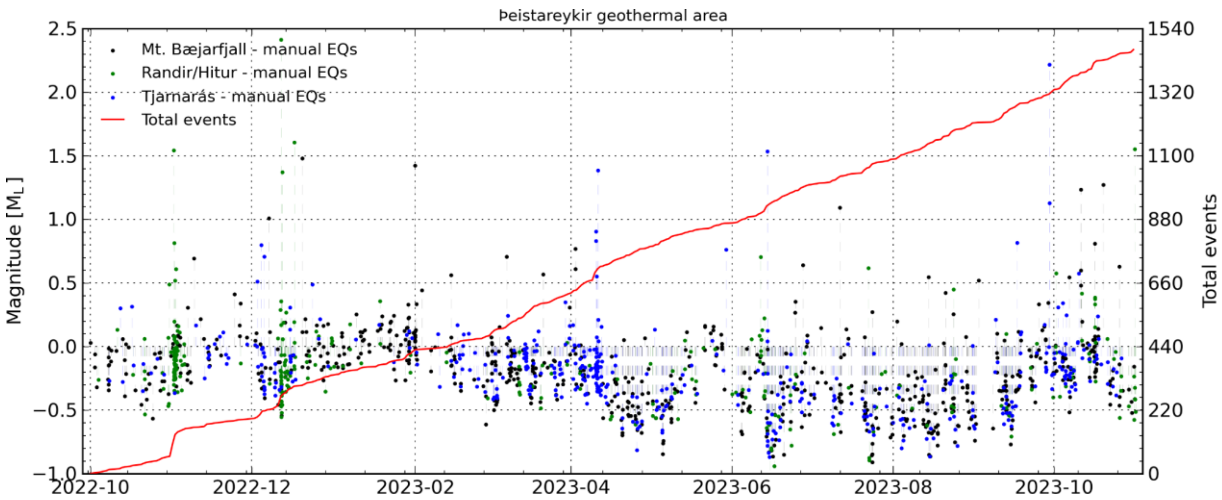

Figure 6. *Time vs. magnitude (M_L) plot of the 1,471 located earthquakes in the Þeistareykir geothermal area (box A in Figure 1) during the study period. Manual earthquakes are shown as different coloured dots, referring to the three different clusters of Bæjarfjall (black), Randir/Hitur (green) and Tjarnarás (green) (see Figures A1 and A2 in Appendix A). The red line shows the cumulative number of earthquakes.*

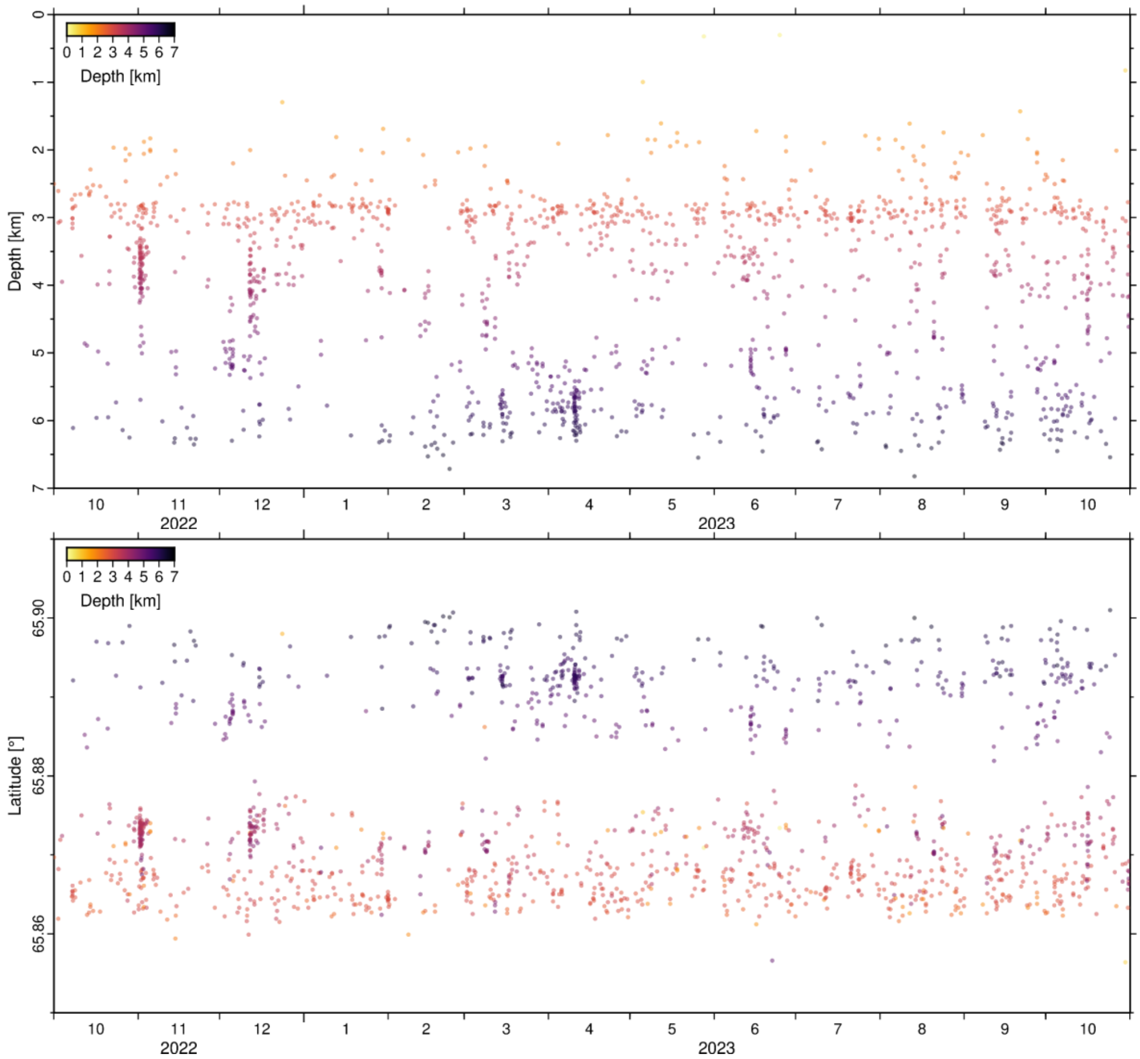

Figure 7. *Time vs. depth (top) and latitude (bottom) of located earthquakes in the Þeistareykir geothermal area (box A in Figure 1) during the study period. Earthquakes are colour-coded by depth.*

3.3 Námafjall

Earthquake activity in the Námafjall geothermal area occurs in a rather scattered cluster within the depth range of 2-6 km during the study period (Figure 8). The majority of earthquakes are confined to one cluster within the well field at a limited depth interval of 3-3.5 km. Other events during the study period are more scattered and fade north into the fissure swarm.

Magnitudes

Magnitudes in Námafjall during the study period range from M_L -0.4 to 1 (Figure 9). As in Krafla and Þeistareykir, seasonal fluctuations are observed in the magnitude distribution, although the earthquakes are few, with smaller earthquakes detected during summer than during winter.

Rate

Looking at Figure 9, it is evident that the low micro-seismic activity in the Námafjall geothermal area is characterised by a rather constant activity, although the rate is slightly higher during the winter months throughout May. It should be noted though, that the LV/ÍSOR seismic network is least sensitive in this area.

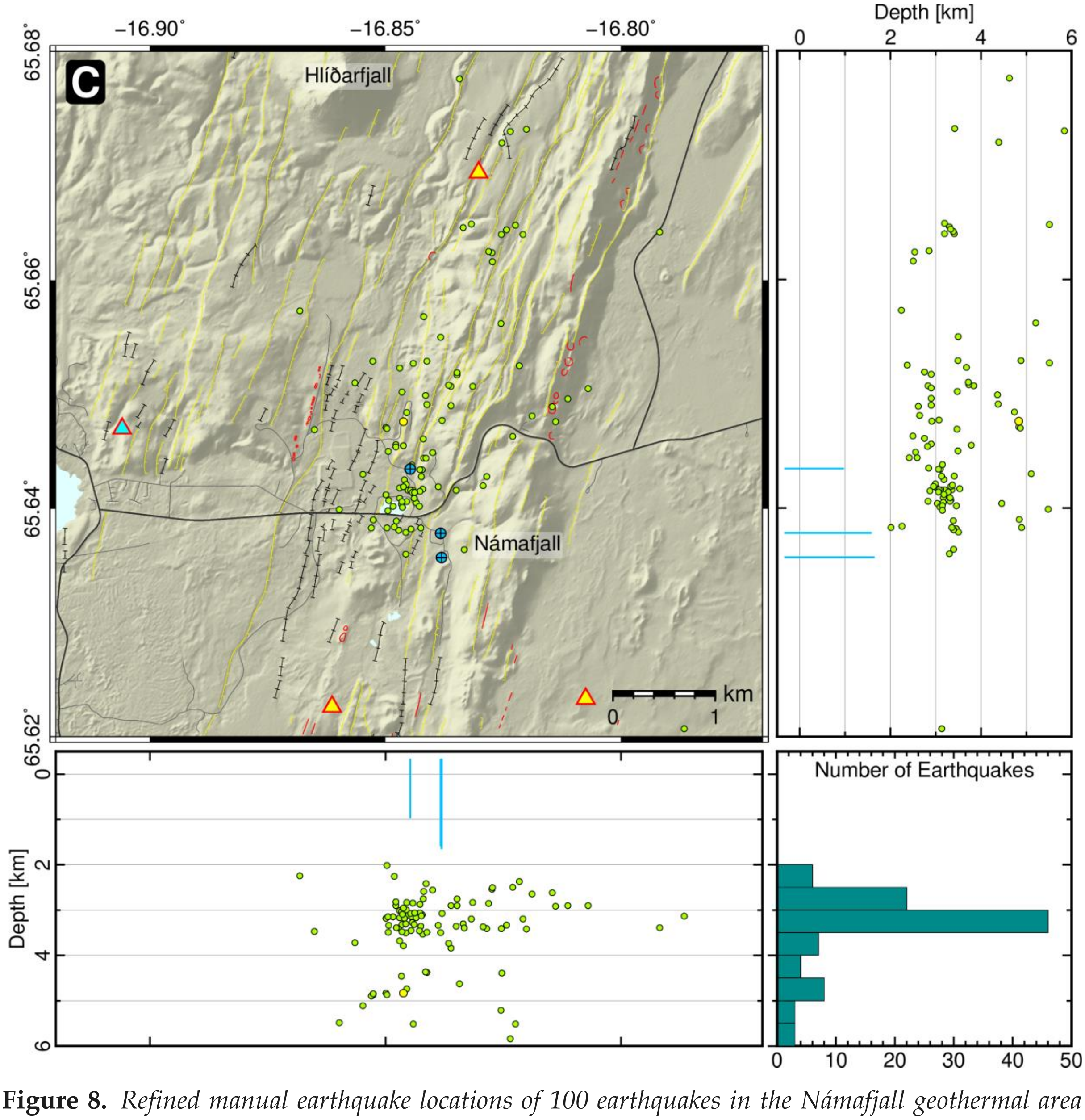

Figure 8. *Refined manual earthquake locations of 100 earthquakes in the Námafjall geothermal area (box C in Figure 1) during the study period, in map and depth view. See legend and figure caption from Figure 1 for references to the map.*

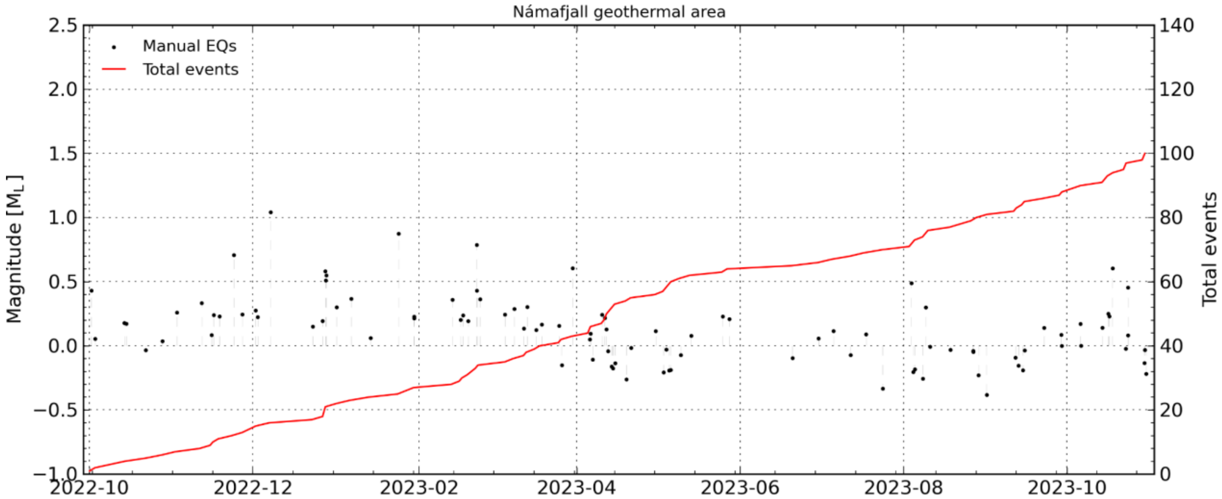

Figure 9. *Time vs. magnitude (M_L) plot of the 100 located earthquakes in the Námafjall geothermal area (box C in Figure 1) during the study period. Manual earthquakes are shown as black dots, and the red line shows the cumulative number of earthquakes.*

4 Focal mechanisms

Earthquake source mechanisms, or focal mechanisms, are either double-couple, or non-double-couple. A double-couple earthquake is caused by shear slip along a planar fault surface (approximated by a point source), where the fault orientation is usually described by strike and dip, and then rake is used to specify the direction of the slip along the fault plane. The double-couple focal mechanism has two nodal planes, but without further information, e.g., geological, it is not possible to distinguish which of the two nodal planes represents the fault plane of the earthquake. Non-double-couple earthquakes are explained in chapter 4.1.

Focal mechanisms presented in this report are calculated using the MTfit inversion software (Pugh and White, 2018). These are full moment tensor inversions using the P-wave polarity phases and take-off angles in the calculations. The focal mechanisms are displayed on maps as “beach ball” symbols, which is the stereographic projection on a horizontal plane of the lower half of an imaginary, spherical shell (the focal sphere) surrounding the earthquake source, where a coloured quadrant represents upward motion at a station and a white quadrant represents downward motion.

The T-axis (tension-axis, minimum compression), P-axis (pressure axis, maximum compression) and N-axis (consistent with the intersection of the nodal planes) are orthogonal to each other. T- and P- axes are deviated 45° from the nodal planes. Their azimuth and plunge give additional information on the direction and inclination of faults. The plane defined by the T- and P-axes also contains the normal vectors to the nodal plane, whereof one is the slip vector.

A total of 343 double-couple focal mechanisms were analysed during the study period, or 216 in Krafla, 115 in Þeistareykir and 12 in Námafjall (Figure 10). To investigate focal mechanisms in each area in more detail, a Frohlich categorisation of the mechanisms is used, to give a better overview of the focal mechanism distribution (Figure 11). It is a triangle diagram, where the vertices represent normal, strike-slip and reverse faulting focal mechanisms using the plunge of the N-, T- and P-axis (Frohlich, 1992). The focal mechanisms in each area are coloured according to the categorisation, i.e., red colour denotes normal faulting, purple strike-slip faulting, orange reverse faulting, and the oblique events are denoted in yellow (Figures 12-17).

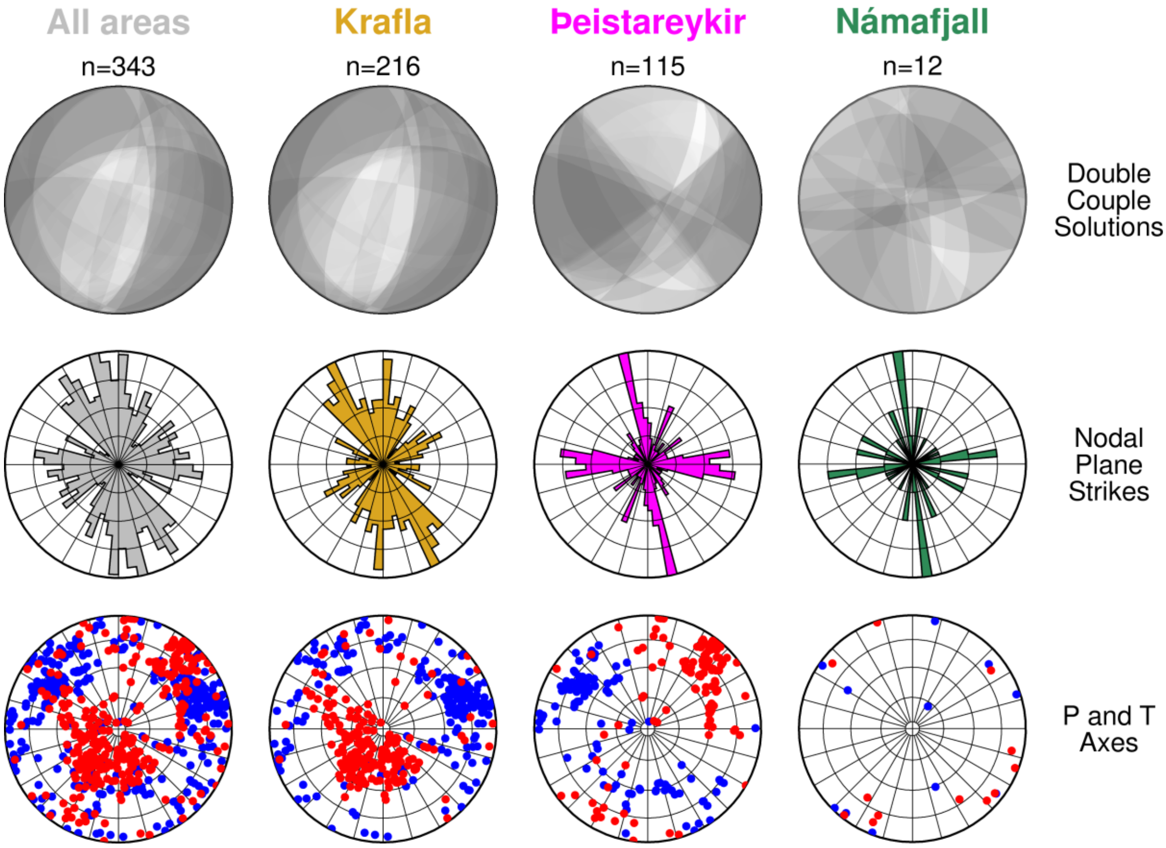

Figure 10. *Graphic summary of all 343 double-couple focal mechanisms located in Krafla, Þeistareykir and Námafjall geothermal areas during the study period, where n equals number of earthquakes in each group. Top row: all focal mechanisms (white dilatation, grey compression), middle row: strike orientation of all nodal planes, bottom row: orientation of the maximum (P-axis (pressure-axis), red dots) and minimum (T-axis (tension-axis), blue dots) compressive stress.*

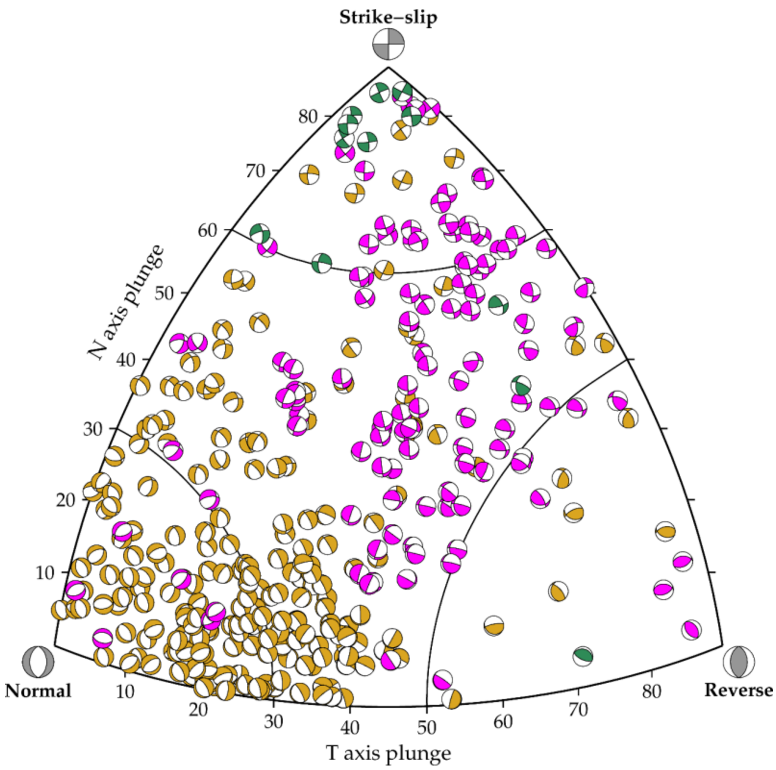

Figure 11. *A Frohlich mechanism categorisation plot (Frohlich, 1992), for all 343 double-couple focal mechanisms displayed in Figure 10. The Frohlich plot is a triangle diagram where the vertices represent normal, strike-slip and reverse focal mechanisms. The different colours refer to the colouring of each geothermal area, as in Figure 10.*

4.1 Krafla

Figures 12 and 13 show the 216 high-quality double-couple focal mechanisms calculated for Krafla during the study period, in map view and the Frohlich categorisation of each event. As before, focal mechanisms in Krafla, particularly within the well field, are dominated by normal faulting to oblique normal faulting, both parallel and perpendicular to the fissure swarm (red and yellow colours in Figures 12 and 13), with steep P-axis and shallow T-axis plunge (red and blue dots, respectively, bottom panel in Figure 10) meaning that most of the normal faults are near vertical. This is in agreement with the catalogue of well constrained focal mechanisms calculated for Krafla from 2018 to 2022, with a total of 640 events (Guðnason et al., 2023).

Although normal faulting is expected within a caldera regime, more strike-slip focal mechanisms are expected to be found within the fissure swarm itself. The few strike-slip to oblique strike-slip events observed in Krafla, both during the study period and in previous years, are mostly confined to the fissure swarm, likely of natural origin. Compared to Þeistareykir and Námafjall, much fewer strike-slip to oblique strike-slip events are observed, meaning that the stress regime in Krafla is very different to both Þeistareykir and Námafjall.

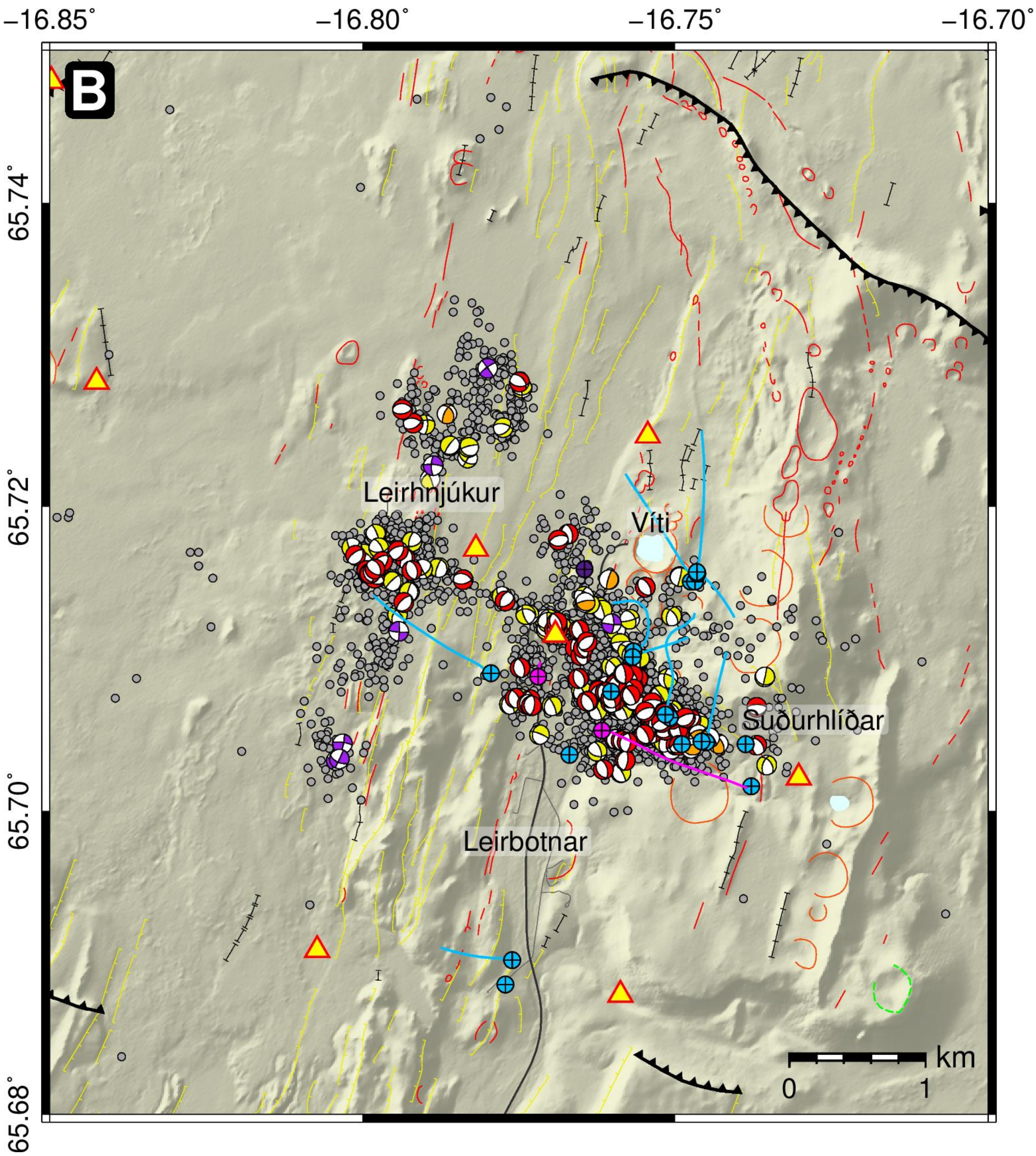

Figure 12. *Map view of double-couple focal mechanisms for 216 selected events in the Krafla geothermal area during the study period, which are dominated by normal faulting to oblique normal faulting, mainly within the Krafla well field. The different colours refer to the colouring for each focal mechanism type (see Figure 13).*

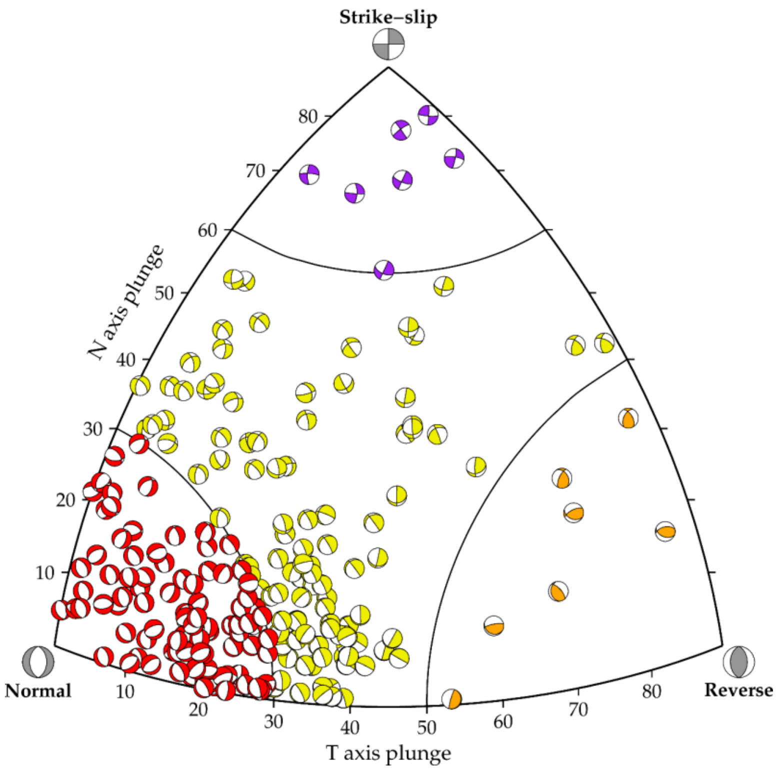

Figure 13. *A Frohlich focal mechanism categorisation plot for the 216 double-couple focal mechanisms in Krafla, displayed in map view in Figure 12. The different colours refer to the colouring for each focal mechanism type.*

4.2 Þeistareykir

Figures 14 and 15 show the 115 high-quality double-couple focal mechanisms calculated for Þeistareykir during the study period, in map view and the Frohlich categorisation of each event. Different to Krafla, focal mechanisms in Þeistareykir are dominated by strike-slip to oblique strike-slip faulting, mainly confined to the Mt. Bæjarfjall cluster (purple and yellow colours in Figures 14 and 15). This is in agreement with the catalogue of well constrained focal mechanisms calculated for Þeistareykir from 2017 to 2022, with a total of 258 events (Guðnason et al., 2023).

The increased seismicity within both the Randir/Hitur and the Tjarnarás clusters made it possible to calculate a higher number of focal mechanisms for these two clusters, compared to previous years (Figure 14). Normal faulting events in Þeistareykir (red colour in Figures 14 and 15) are exclusively confined to the Randir/Hitur cluster during the study period, which is in good agreement with the catalogue of focal mechanisms from previous years (Guðnason et al., 2023). The Randir/Hitur cluster also comprises oblique normal and strike-slip faulting events during the study period. The Tjarnarás cluster is mainly characterised by strike-slip to oblique strike-slip faulting events, with some reverse faulting events in between. In general, no significant change is observed in faulting mechanisms within these two clusters of the fissure swarm, compared to previous years, despite the ongoing inflation (Guðnason et al., 2023).

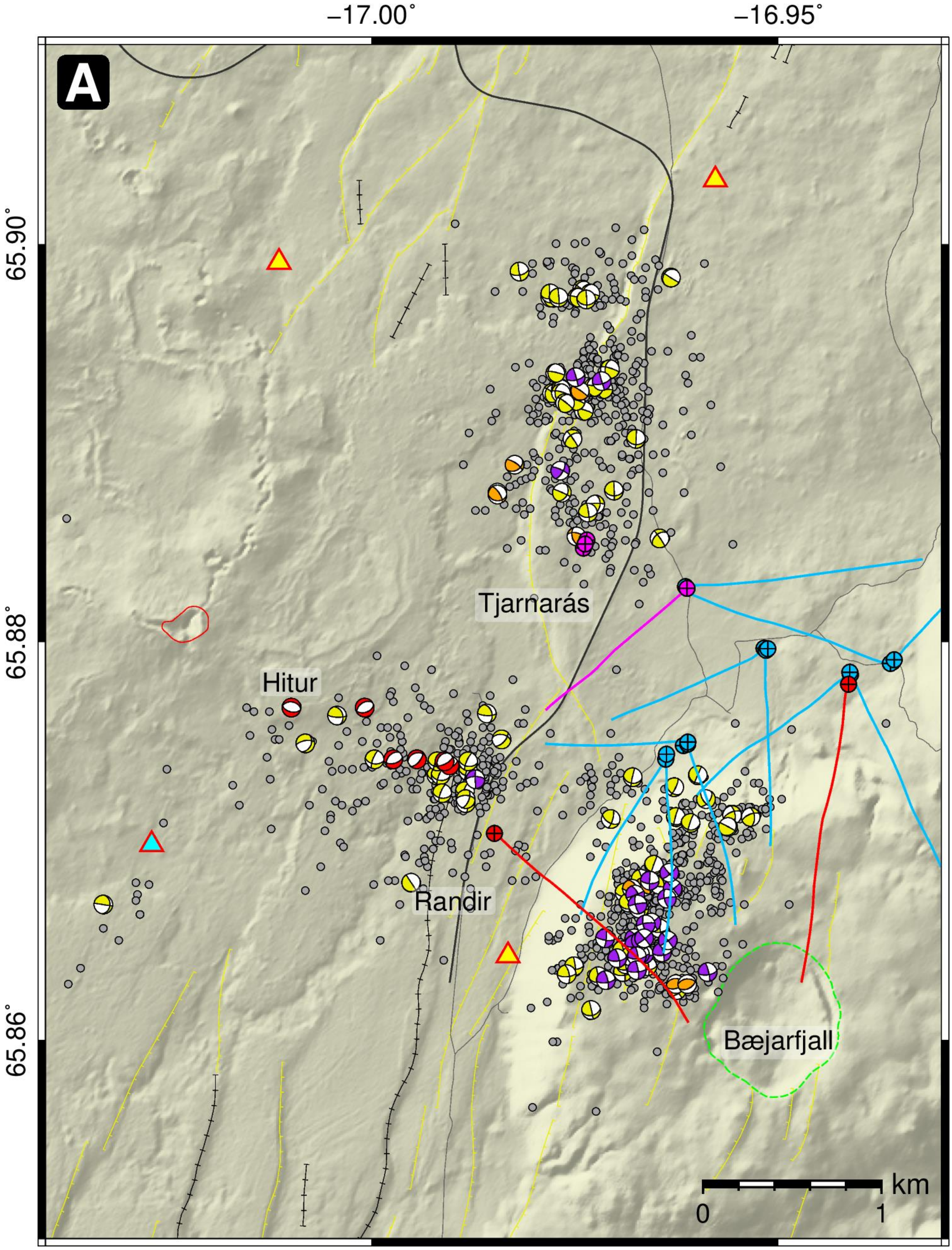

Figure 14. *Map view of double-couple focal mechanisms for 115 selected events in the Þeistareykir geothermal area during the study period, which are dominated by strike-slip to oblique strike-slip faulting, mainly within the Mt. Bæjarfjall cluster. The different colours refer to the colouring for each focal mechanism type (see Figure 15).*

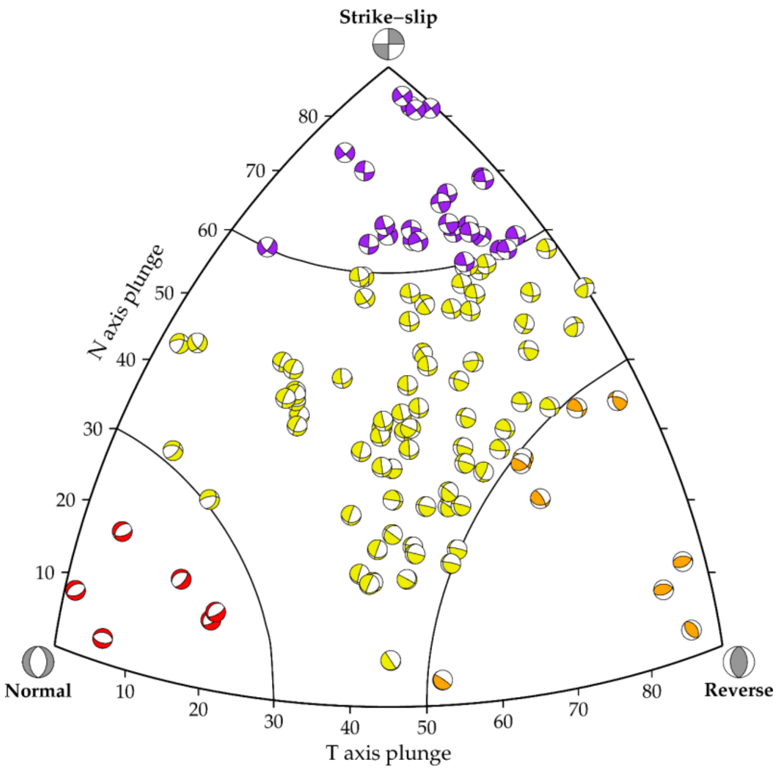

Figure 15. *A Frohlich focal mechanism categorisation plot for the 115 double-couple focal mechanisms in Þeistareykir, displayed in map view in Figure 14. The different colours refer to the colouring for each focal mechanism type.*

4.3 Námafjall

Figures 16 and 17 show the 12 double-couple focal mechanisms calculated for Námafjall during the study period, in map view and the Frohlich categorisation of each event. In Námafjall, the focal mechanisms are less constrained than in Krafla and Þeistareykir, mainly due to the sparse station coverage. Due to the network configuration, focal mechanisms in Námafjall can quite easily shift between oblique strike slip and reverse earthquakes as the nodal planes are not tightly constrained.

Focal mechanisms in Námafjall are dominated by strike-slip faulting (purple colour in Figures 16 and 17), likely dominated by the fissure swarm. This is in agreement with the catalogue of focal mechanisms calculated for Námafjall from 2019 to 2022, with a total of 29 events (Guðnason et al., 2023).

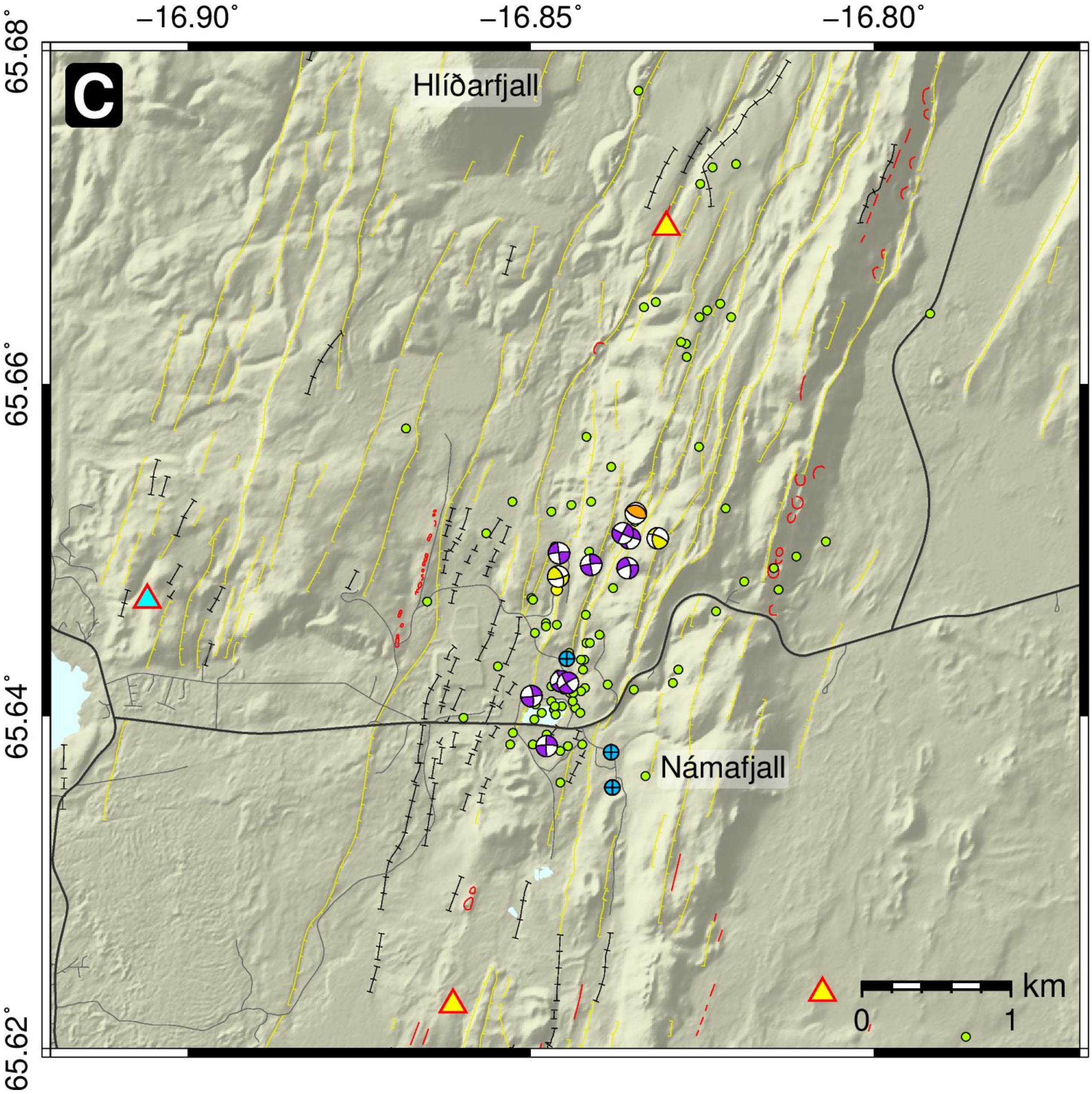

Figure 16. *Map view of double-couple focal mechanisms for 12 selected events in the Námafjall geothermal area during the study period, which are dominated by strike-slip to oblique strike-slip faulting. The different colours refer to the colouring for each focal mechanism type (see Figure 17).*

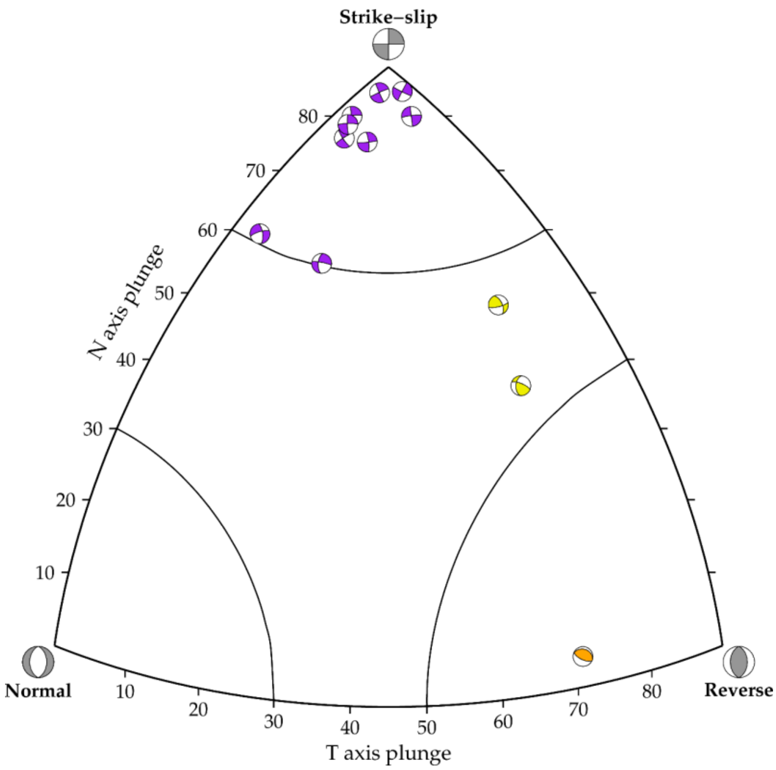

Figure 17. *A Frohlich focal mechanism categorisation plot for the 12 double-couple focal mechanisms in Námafjall, displayed in map view in Figure 16. The different colours refer to the colouring for each focal mechanism type.*

4.4 Non-double-couple earthquakes

The radiation pattern of seismic waves from some earthquakes cannot be produced by shear slip along a planar fault surface. Instead of shear slip, these earthquakes are caused by a volumetric change and are referred to in the literature as non-double-couple. Shallow, non-double-couple earthquakes have been observed within volcanic and geothermal areas, e.g., in Iceland, and more importantly in Krafla (Foulger and Long, 1984; Arnott and Foulger, 1994; Mildon et al., 2016; Schuler et al., 2016; Guðnason et al., 2023). They require explanations such as involvement of fluids, slip along curved faults or fractal faulting as possible causes (Frohlich, 1994).

During the study period, 35 earthquakes in Krafla are observed which are consistent with a pure non-shear faulting behaviour (Figure 18). Event magnitudes are in the range of M_L -0.11 to 0.93. An earthquake is only classified as pure non-double-couple if all P-wave polarities are identical, i.e., either positive or negative. These are non-shear faulting mechanisms that involve either positive or negative volume change, referred to as explosive (positive P-wave polarities) and implosive (negative P-wave polarities) events, respectively. Out of 35 earthquakes, 23 are explosive and 12 are implosive. Two events are observed where one P-wave polarity is non-identical to the rest, and thus, identified as a non-double-couple event, as it did not fit a double-couple inversion.

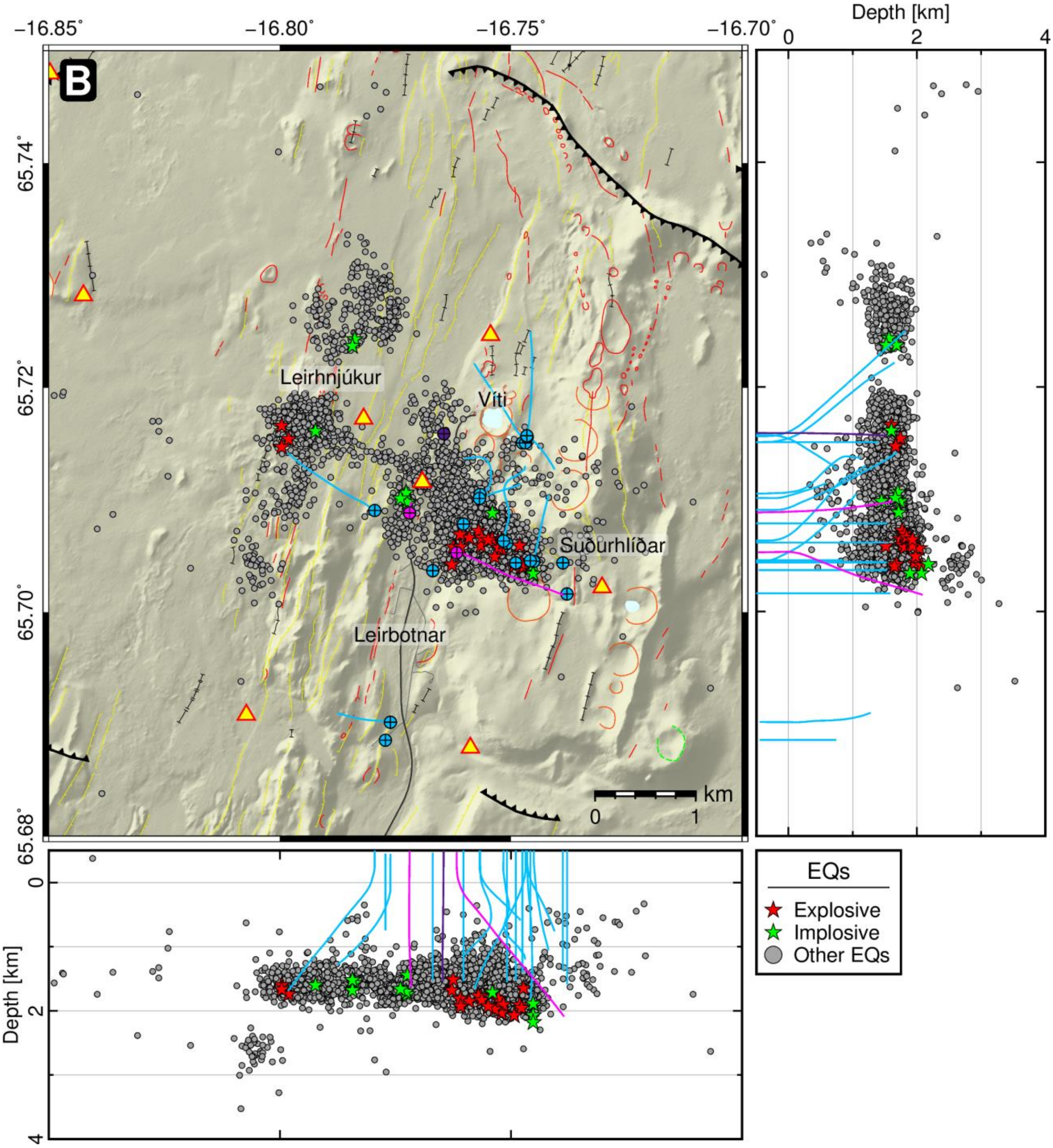

Figure 18. *Pure non-double-couple earthquakes in the Krafla geothermal area (box B in Figure 1) during the study period, in map and depth view. Explosive events are marked with a red star, and implosive events are marked with a green star.*

Non-double-couple earthquakes in Krafla have been studied in detail since 2020 (Guðnason et al., 2023). During the study period, implosive events are observed for the first time within the northernmost cluster of the Krafla fissure swarm. As observed between 2020 and 2022 (Figure B1 in Appendix B) (Guðnason et al., 2023), there are two interesting observations from Figure 18;

i. All non-double-couple earthquakes observed in Krafla occur at the deeper end of the depth range, i.e., close to or at the brittle-ductile transition, or the expected melt-rock interface, where magma has already been encountered. This suggests that geothermal fluids play an important role in their source processes.

ii. The explosive and implosive events are divided between the southern and central part of the Krafla well field, but also between the southern and northern part of the Krafla fissure swarm. This division, also observed by Schuler et al. (2016), suggests some changes within the geothermal reservoir of Krafla, which needs further study.

The total of 84 non-double-couple earthquakes observed in Krafla, from 2020 to 2023, are shown in Appendix B (Figure B1). Non-double-couple earthquakes in Krafla occur at a depth where geothermal fluid can change the stress locally, and cracks may either open (explosive) or close (implosive). In agreement with previous studies of non-double-couple earthquakes within geothermal areas in Iceland, we find that double-couple and non-double-couple earthquakes are interspersed laterally.

5 Vp/Vs ratio

Seismic wave velocities, both P-wave (Vp) and S-wave (Vs), are fundamental seismic properties. Seismic velocities generally increase with depth, although they vary with changes in both internal and external conditions as e.g., confining stress, temperature, pore pressure, fluid saturation, porosity, and crack density (Hersir et al., 2022).

Consequently, the Vp/Vs ratio provides information on e.g., rock properties and phase change of fluids present in the rock, and changes in the ratio are associated with the elastic parameters of the crust, as well as with porosity, pore filling and stress state (Nur, 1987; Jousset et al., 2011 and references therein).

The Vp/Vs ratio for the Krafla, Þeistareykir and Námafjall geothermal areas is estimated using standard Wadati diagrams (Wadati, 1933). In a Wadati diagram, the difference of the S- and P-wave travel times is plotted as a function of the P-wave travel time. The relationship between the two should be linear, and the slope of the best fitting line, determined with linear regression, gives a reasonable estimate of the Vp/Vs ratio in the sampled crust for each geothermal area (Figure 19). The ratio averages over the whole travel paths of seismic waves for individual earthquakes. To ensure that the calculated Vp/Vs ratio is representative of the crust within each area, only earthquakes and seismic stations within each of the marked black boxes in Figure 1 (A-C) are used.

The calculated Vp/Vs ratio during the study period is 1.73 ± 0.01 in Krafla, 1.77 ± 0.01 in Þeistareykir and 1.73 ± 0.09 in Námafjall (Figure 19 and Table 1). The Vp/Vs ratio was not calculated in last year's report, covering the time period from the 1st of October 2021 to the 30th of September 2022 (Guðnason et al., 2022), and thus it is calculated and included now (Table 1 and Figure C1 in Appendix C).

The Vp/Vs ratio in all three geothermal areas; Krafla, Þeistareykir and Námafjall, has been continuously analysed since 2016 (Guðnason et al., 2021 and references therein) (Table 1). Between 2016 and 2021, the ratio of 1.70-1.71 in Krafla remained the same within the uncertainty limit. However, the Vp/Vs ratio in Krafla increases slightly during 2022 and 2023, which needs further attention. The ratios in Þeistareykir and Námafjall are a little higher and more variable, varying between 1.72 and 1.77 in Þeistareykir and 1.72 and 1.78 in Námafjall. The ratio in Þeistareykir, and especially in Námafjall, is based on an order of magnitude smaller number of earthquakes than in Krafla. The Vp/Vs ratio variations in Þeistareykir and Námafjall, therefore, have to be regarded with caution.

The ratio in all three areas is lower than the ratio of 1.78, which is typically observed in the Icelandic crust (Brandsdóttir and Menke, 2008). A low Vp/Vs ratio might indicate a phase change from liquid to steam, the presence of supercritical pore fluid, or extremely fractured medium (Ito et al., 1979; Hersir et al., 2022).

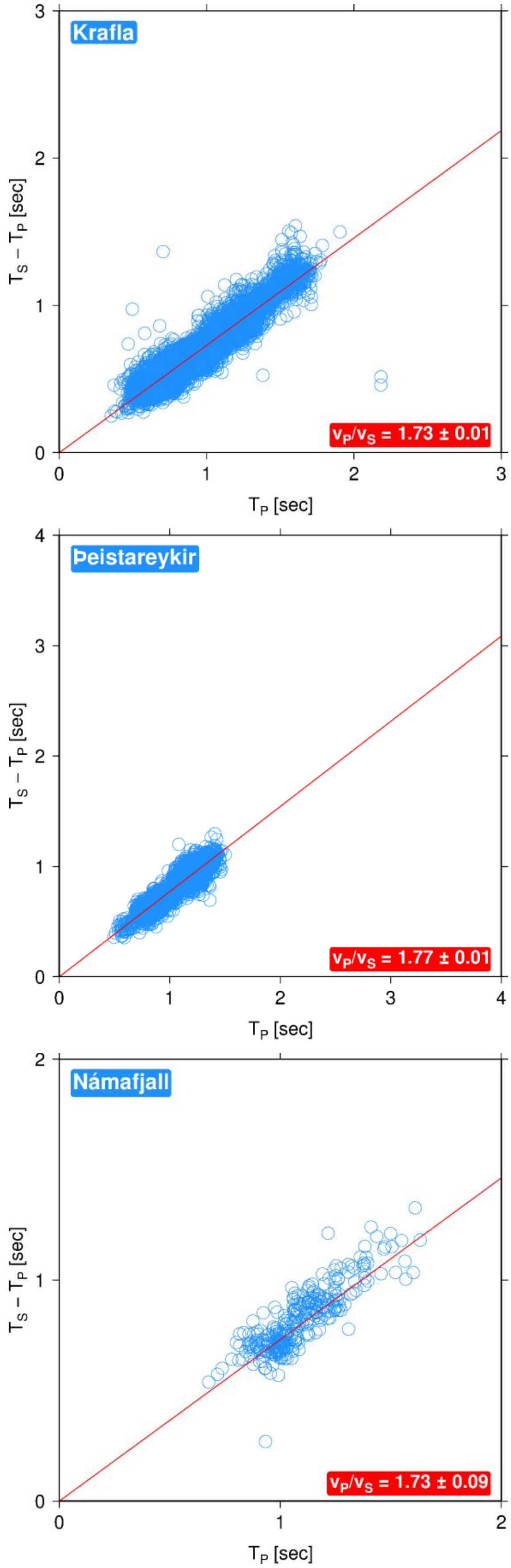

Figure 19. *Calculated Vp/Vs ratio for the Krafla, Þeistareykir and Námafjall geothermal areas during the study period, from top to bottom, respectively.*

Table 1. *Calculated Vp/Vs ratio for the Krafla, Þeistareykir and Námafjall geothermal areas from 2016-2017 to 2022-2023 (Guðnason et al., 2021 and references therein).*

	Krafla	Þeistareykir	Námafjall
2016-2017	1.70 ± 0.01	1.72 ± 0.02	1.72 ± 0.02
2017-2018	1.70 ± 0.01	1.76 ± 0.01	1.72 ± 0.01
2018-2019	1.71 ± 0.01	1.74 ± 0.01	1.76 ± 0.01
2019-2020	1.71 ± 0.01	1.72 ± 0.01	1.78 ± 0.02
2020-2021	1.71 ± 0.01	1.75 ± 0.01	1.73 ± 0.12
2021-2022	1.72 ± 0.01	1.72 ± 0.01	1.77 ± 0.09
2022-2023	1.73 ± 0.01	1.77 ± 0.01	1.73 ± 0.09

6 Conclusions

Seismic monitoring by Landsvirkjun and ÍSOR of the three developed high-temperature geothermal areas of the Northern Volcanic Zone, NE Iceland; Krafla, Þeistareykir and Námafjall, has provided a large and interesting dataset, i.e., a complete and consistent catalogue of around 70,000 earthquakes, which enables us to reliably look at long term changes in seismicity in all three areas. The main goal is to monitor seismic activity associated with the utilisation of, and re-injection into, the three respective geothermal systems, as well as to monitor natural activity in these volcanic environments.

Results of this year's monitoring are:

- From the 1st of October 2022 to the 31st of October 2023, a total of 5,275 earthquakes were located in the Krafla, Þeistareykir and Námafjall geothermal areas and surroundings, with the highest concentration of earthquakes in Krafla.
- The observed seismicity rate in Krafla and Námafjall is similar to last year, while there is a significant increase in Þeistareykir, both within the Randir/Hitur and the Tjarnarás cluster. The increase within the Tjarnarás cluster coincides with the start of an inflation in Þeistareykir, and is therefore most likely a crustal response to the ongoing inflation in the area.
- Micro-seismicity is dominant in all three geothermal areas, with 99% of earthquakes of $M_L < 1.0$, and only three events exceeding M_L 2.0.
- Seasonal variations are observed in i) the seismicity rate in Krafla and Námafjall, with higher rates during the winter months, and in ii) the magnitude range in all three areas, with smaller earthquakes detected during summer, than during winter.
- Drilling and stimulation of two new wells below Mt. Bæjarfjall in Þeistareykir in 2023, wells ÞG-19 and ÞG-20, did not induce any significant earthquake activity, further confirming the theory that the Mt. Bæjarfjall cluster is of natural origin.
- Double-couple focal mechanisms are calculated for a total of 343 earthquakes, or 216 in Krafla, 115 in Þeistareykir and 12 in Námafjall. Diverse faulting styles are inferred,

with normal faulting dominant in Krafla, while strike-slip faulting is dominant in both Þeistareykir and Námafjall.

    - No significant change is observed in faulting mechanisms within the Tjarnarás cluster in Þeistareykir compared to previous years, despite the ongoing inflation.

- 35 earthquakes in Krafla are attributed to pure non-double-couple mechanisms, both explosive and implosive. As before, they are located at the expected melt-rock interface, close to the brittle-ductile transition.
    - From 2020 to 2023, explosive and implosive events are divided between the southern and central part of the Krafla well field, and to some extent between the southern and northern part of the Krafla fissure swarm.
- The calculated Vp/Vs ratio from 2021 to 2023 in all three areas is relatively low, compared to standard values of the Icelandic crust. The ratio in Krafla increases slightly, compared to 2016-2021, while the ratios in Þeistareykir and Námafjall are a little higher, and more variable from year to year.

References

Arnott, S., and Foulger, G. (1994). The Krafla spreading segment, Iceland: 2. The accretionary stress cycle and nonshear earthquake focal mechanisms. *J. Geophys. Res.*, *99*, 23, 827–23,842. https://doi.org/10.1029/94JB00688.

Ágústsson, K. and Flóvenz, Ó. G. (2005). The Thickness of the Seismogenic Crust in Iceland and its Implications for Geothermal Systems. *Proceedings of the World Geothermal Congress 2005, Antalya, Turkey*, 9 p.

Ágústsson, K., Guðnason, E. Á., Gunnarsson, K. and Árnadóttir, S. (2011). *Skjálftaverkefnið í Kröflu: Staðan í júní 2011*. Iceland GeoSurvey, short report, ÍSOR-11064.

Árnadóttir, S., Mortensen, A. K., Gautason, B., Ingimarsdóttir, A., Massiot, C., Jónsson, R. B., Sveinbjörnsson, S., Tryggvason, H. H., Egilson, Þ., Eiríksson, J. E. and Haraldsson, K. (2009). *Krafla – Leirbotnar. Hola KJ-39. 3. áfangi: Borsaga.* Iceland GeoSurvey, ÍSOR-2009/058, LV-2009-128, 170 p.

Bali, E., Aradi, L. E., Zierenberg, R., Diamond, L. W., Pettke, T., Szabó, Á., Guðfinnsson, G. H., Friðleifsson, G. Ó. and Szabó, C. (2020). Geothermal energy and ore-forming potential of 600°C mid-ocean ridge hydrothermal fluids. *Geology*, *48 (12),* 1221-1225. https://doi.org/-10.1130/G47791.1.

Blischke, A., Níelsson, S. and Kaldal, G. S. (2023). *Þeistareykir Geothermal Field: Geological Borehole Prognosis for Wells ÞG-19 and ÞG-20 of Bæjarfjall.* Iceland GeoSurvey, Short Report, ÍSOR-23004, 7 p. (with two appendices).

Brandsdóttir, B. and Menke, W. (2008). The seismic structure of Iceland, *Jökull*, *58*, 17–34. http://dx.doi.org/10.33799/jokull2008.58.017.

Drouin, V. (2023). *InSAR monitoring of Krafla, Bjarnarflag and Þeistareykir geothermal areas – 2023 update.* Landsvirkjun, LV-2023-063, 25 p.

Einarsson, P. (1991). The Krafla rifting episode 1975-1989 in *Náttúra Mývatns* (eds.) Garðarsson, A. and Einarsson, A. Reykjavík: Icelandic Nature Science Society, 97-139.

Flóvenz, Ó. G., Drouin, V., Ágústsson, K., Guðnason, E. Á., Hersir, G. P., Ágústsdóttir, T. and Magnússon, I. Þ. (2020). The Interaction of the Plate Boundary Movement in 2020 and Exploitation of Geothermal Fields on the Reykjanes Peninsula, Iceland. *Proceedings of the World Geothermal Congress 2020+1*, Reykjavík, Iceland, 14 p.

Foulger, G. R. and Long, R. E. (1984). Anomalous focal mechanisms: Tensile crack formation on an accreting plate boundary. *Nature*, *310*, 43–45. https://doi.org/10.1038/310043a0.

Frohlich, C. (1992). Triangle diagrams: ternary graphs to display similarity and diversity of earthquake focal mechanisms. *Physics of the Earth and Planetary Interiors*, *75*, 193-198. https://doi.org/10.1016/0031-9201(92)90130-N.

Frohlich, C. (1994). Earthquakes with non-double-couple mechanisms. *Science*, *264*, 804–809. https://doi.org/10.1126/science.264.5160.804.

Guðnason, E. Á. and Ágústsdóttir, Þ. (2021). *Þeistareykir. Minimum 1D Velocity Model*. Iceland GeoSurvey, ÍSOR-2021/003, LV-2021-002, 36 p.

Guðnason, E. Á. and Ágústsdóttir, Þ. (2023). *Earthquake Activity in Þeistareykir October to December 2022.* Iceland GeoSurvey, Short Report, ÍSOR-23011, 9 p.

Guðnason, E. Á., Ágústsdóttir, Þ., Magnússon, R. L. and Gunnarsson, K. (2022). *Seismic Monitoring in Krafla, Þeistareykir and Námafjall. October 2021 to October 2022.* Iceland GeoSurvey, ÍSOR-2022/049, LV-2022-057, 42 p.

Guðnason, E. Á., Ágústsdóttir, Þ., Magnússon, R. L. and Gunnarsson, K. (2023). *Seismic Monitoring in Krafla, Þeistareykir and Námafjall. Reprocessing of the Entire 2006-2022 Catalogue.* Iceland GeoSurvey, ÍSOR-2023/009, LV-2023-021, 56 p.

Guðnason, E. Á., Magnússon, R. L., Vilhjálmsson, A. M., Ágústsdóttir, Þ. and Gunnarsson, K. (2021). *Seismic Monitoring in Krafla, Þeistareykir and Námafjall. November 2020 to November 2021*. Iceland GeoSurvey, ÍSOR-2021/049, LV-2021-053, 56 p. http://gogn.lv.is/files/2021-/2021-053.pdf.

Hersir, G. P., Guðnason, E. Á. and Flóvenz, Ó. G. (2022) Geophysical Exploration Techniques. In: *Letcher, Trevor M. (eds.) Comprehensive Renewable Energy, 2nd edition*, vol. *7*, 26–79. Oxford: Elsevier. https://doi.org/10.1016/b978-0-12-819727-1.00128-x.

Ito, H., DeVilbiss, J. and Nur, A. (1979). Compressional and shear waves in saturated rock during water-steam transition. *J. Geophys. Res.*, *84*, 4731-4735.

Jousset, P., Haberland, C., Bauer, K. and Árnason, K. (2011). Hengill geothermal volcanic complex (Iceland) characterized by integrated geophysical observations. *Geothermics*, *40* (1), 1-24. https://doi.org/10.1016/j.geothermics.2010.12.008.

Jóngeirsdóttir, I. G., Helgadóttir, H. M., Egilson, Þ., Jónsson, J. E., Aðalsteinsson, S. M. and Árnadóttir, S. (2023a). *Þeistareykir – Well ÞG-19. Phase 3: Drilling for 7" Perforated Liner from 1125 m down to 3000 m Depth.* Iceland GeoSurvey, ÍSOR-2023/044, LV-2023-061, 90 p. + daily reports.

Jóngeirsdóttir, I. G., Árnadóttir, S., Egilson, Þ. and Jónsson, J. E. (2023b). *Þeistareykir – Well ÞG-20. Phase 3: Drilling for a 7" Perforated Liner from 1030 m down to 3000 m.* Iceland GeoSurvey, ÍSOR-2023/046, LV-2023-069, in prep.

Kim, D., Brown, L. D., Árnason, K., Gudmundsson, Ó., Ágústsson, K. and Flóvenz, Ó. G. (2020). Magma „bright spots" mapped beneath Krafla, Iceland, using RVSP imaging of reflected waves from microearthquakes. *J. Volc. Geotherm. Res., 391,* 106365. https://doi.org/10.1016/j.jvolgeores.2018.04.022.

Lomax, A., Virieux, J., Volant, P. and Berge-Thierry, C. (2000). *Probabilistic Earthquake Location in 3D and Layered Models*. In: Thurber C.H., Rabinowitz N. (eds.), Advances in Seismic Event Location. Modern Approaches in Geophysics, vol. 18. Springer, Dordrecht. http://dx.doi.org/10.1007/978-94-015-9536-0_5.

Mildon, Z. K., Pugh, D. J., Tarasewicz, J., White, R. S. and Brandsdóttir, B. (2016). Closing crack earthquakes within the Krafla caldera, North Iceland. *Geophys. J. Int.*, *207* (2), 1137-1141. https://doi.org/10.1093/gji/ggw325.

Mortensen, A. K., Egilson, Þ., Gautason, B., Árnadóttir, S. and Guðmundsson, Á. (2014). Stratigraphy, alteration mineralogy, permeability and temperature conditions of well IDDP-1, Krafla, NE-Iceland. *Geothermics*, *49*, 31-41. https://doi.org/10.1016/j.geothermics.-2013.09.013.

Nur, A. (1987). Seismic rock properties for reservoir descriptions and tomography. In: Nolet, G. (ed.), *Seismic Tomography, 237*. Dordrecht, Springer. https://doi.org/10.1007/978-94-009-3899-1_9.

Pugh, D. J. and White, R. S. (2018). MTfit: A Bayesian approach to seismic moment tensor inversion. *Seismol. Res. Lett.*, *89* (4), 1507-1513. https://doi.org/10.1785/0220170273.

Schuler, J., Greenfield, T., White, R. S., Roecker, S. W., Brandsdóttir, B., Stock, J. M., Tarasewicz, J., Martens, H. R. and Pugh, D. (2015a). Seismic imaging of the shallow crust beneath the Krafla central volcano, NE Iceland. *J. Geophys. Res. Solid Earth, 120,* 7156-7173. https://doi.org/10.1002/2015JB012350.

Schuler, J., Pugh, D. J., Hauksson, E., White, R. S., Stock, J. M. and Brandsdóttir, B. (2016). Focal mechanisms and size distribution of earthquakes beneath the Krafla central volcano, NE Iceland. *J. Geophys. Res. Solid Earth*, *121* (7), 5152-5168. https://doi.org/10.1002/2016JB013213.

Schuler, J., White, R. S., Brandsdóttir, B. and Tarasewicz, J. (2015b). Shallow geothermal and deep seismicity beneath Þeistareykir, NE-Iceland. *Jökull*, *65*, 51-59. https://doi.org/-10.33799/jokull2015.65.051.

Sæmundsson, K., Hjartarson, Á., Kaldal, I., Sigurgeirsson, M. Á., Kristinsson, S. G. and Víkingsson, S. (2012). *Jarðfræðikort af Norðurgosbelti – Nyrðri hluti, 1:100.000*. Reykjavík, Iceland GeoSurvey.

Violay, M., Gibert, B., Mainprice, D., Evans, B., Dautria, J.-M., Azais, P. and Pezard, P. (2012). An experimental study of the brittle-ductile transition of basalt at oceanic crust pressure and temperature conditions. *J. Geophys. Res.*, *117*, B03213. http://dx.doi.org/10.1029-/2011JB008884.

Wadati, K. (1933). On travel time of earthquake waves. *Geophys. Mag., 7*, 101–111.

Appendix A: Seismicity in Þeistareykir

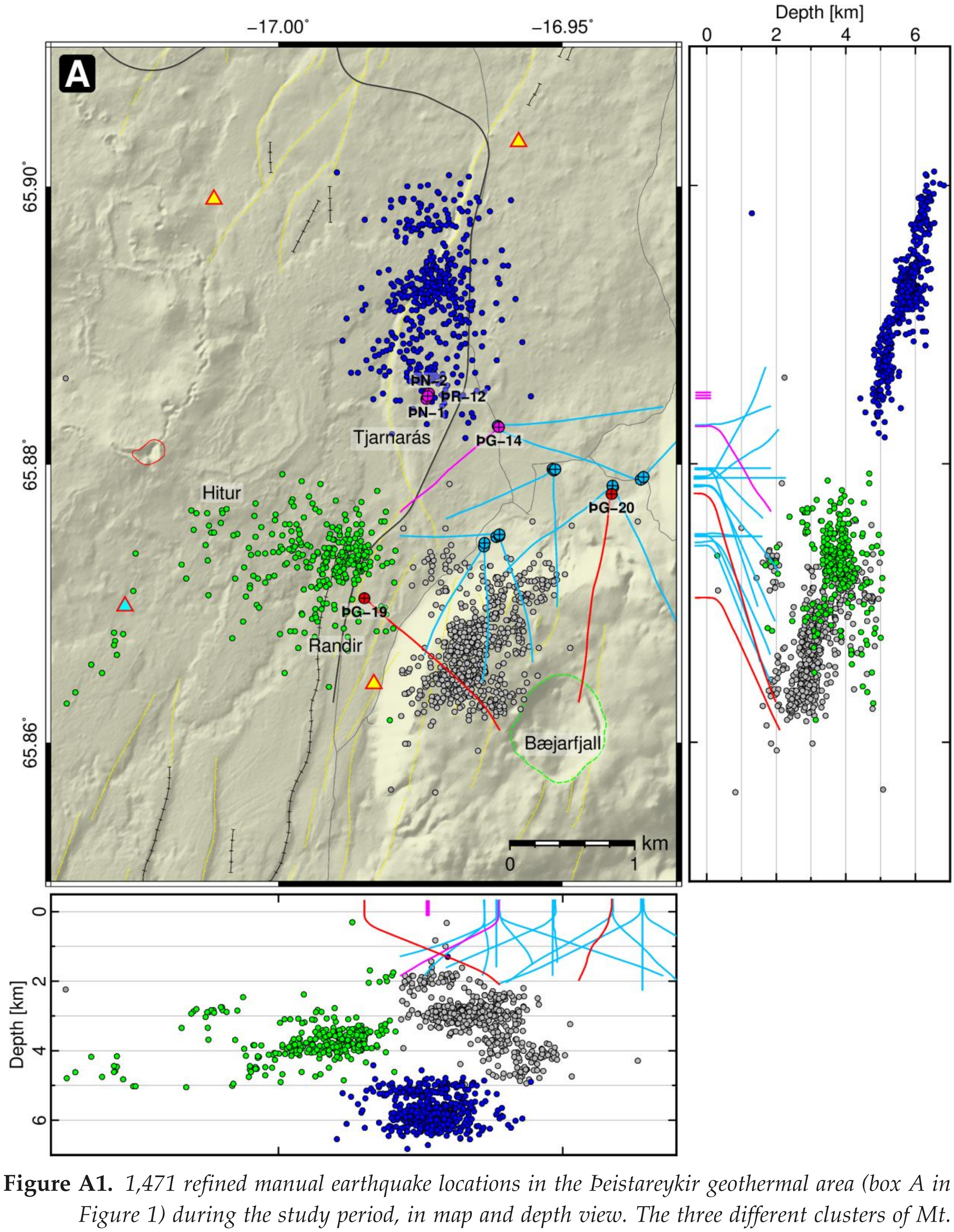

Figure A1. *1,471 refined manual earthquake locations in the Þeistareykir geothermal area (box A in Figure 1) during the study period, in map and depth view. The three different clusters of Mt. Bæjarfjall, Randir/Hitur and Tjarnarás are shown in different colours; grey, green and blue, respectively. The two new wells, ÞG-19 and ÞG-20, are highlighted in red colour.*

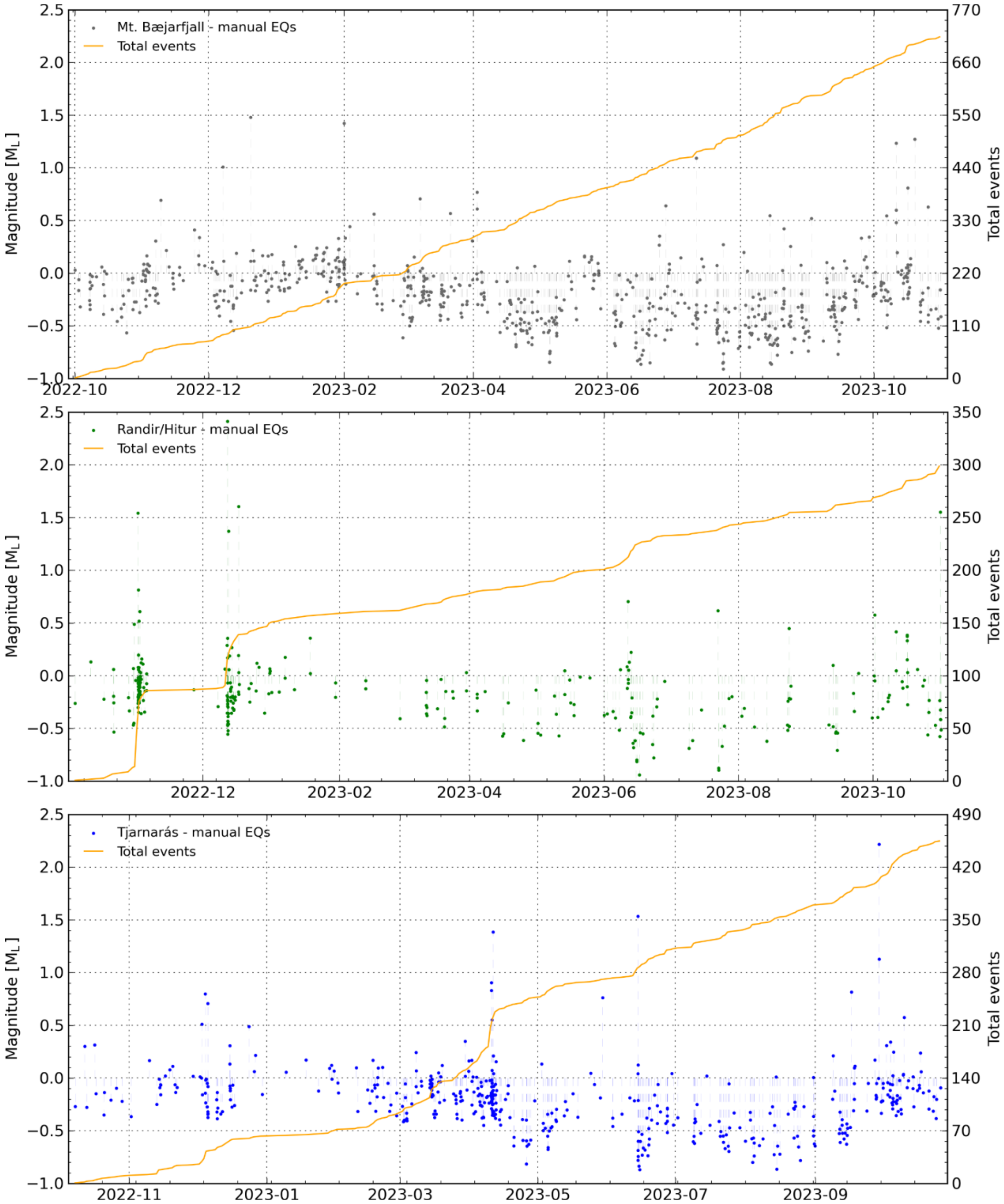

Figure A2. *Time vs. magnitude (M_L) plots of the three different earthquake clusters in the Þeistareykir geothermal area during the study period. Manual earthquakes are shown as different coloured dots, with reference to Figure A1; the Mt. Bæjarfjall cluster in grey (top), the Randir/Hitur cluster in green (middle) and the Tjarnarás cluster in blue (bottom). The orange line in all plots shows the cumulative number of earthquakes in each separate cluster.*

Appendix B: Non-double-couple earthquakes in Krafla

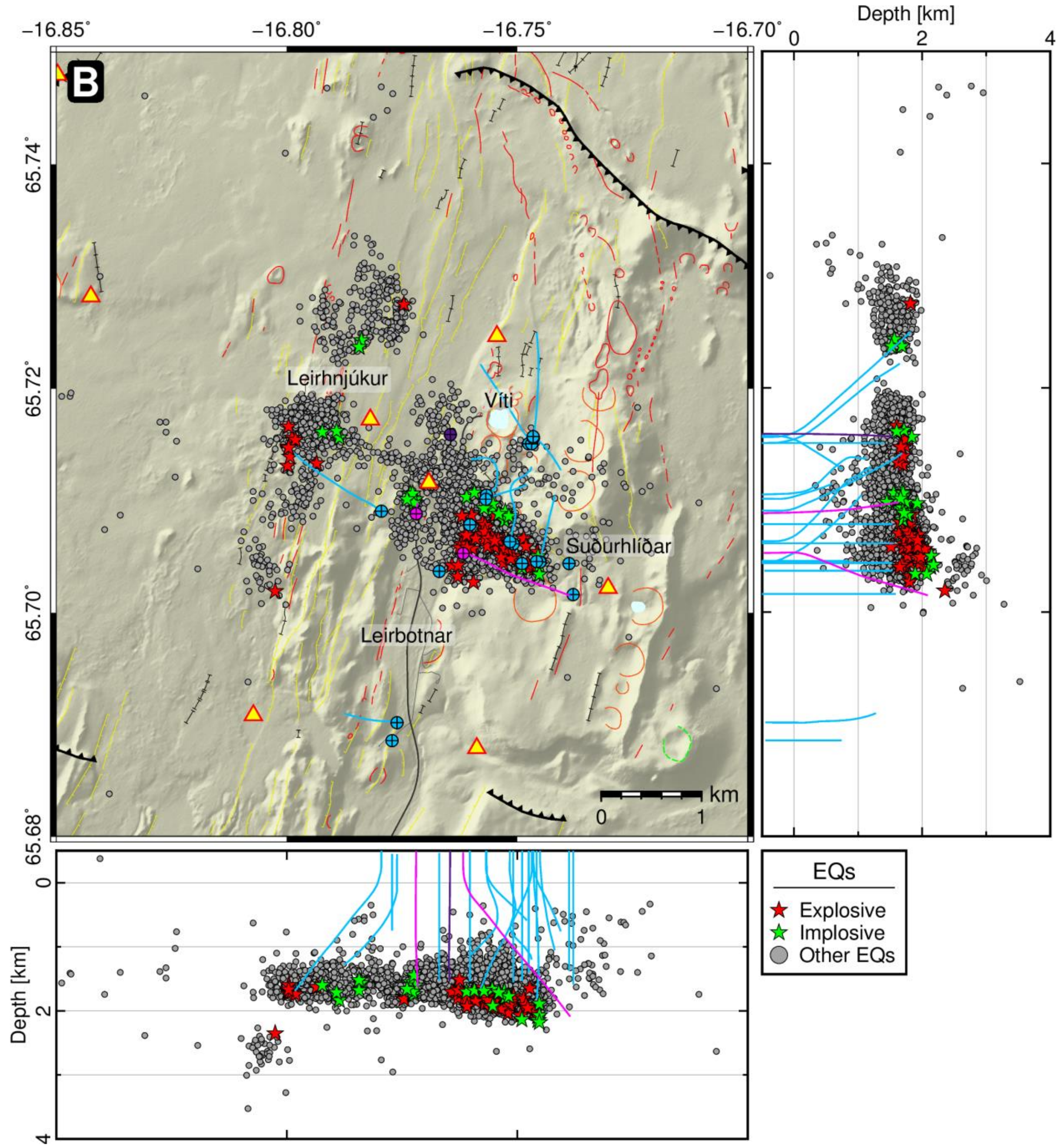

Figure B1. *Non-double-couple earthquakes in the Krafla geothermal area (box B in Figure 1) from 2020-2023, in map and depth view. Explosive events are marked with a red star, and implosive events are marked with a green star.*

Appendix C: Vp/Vs ratio for 2021-2022

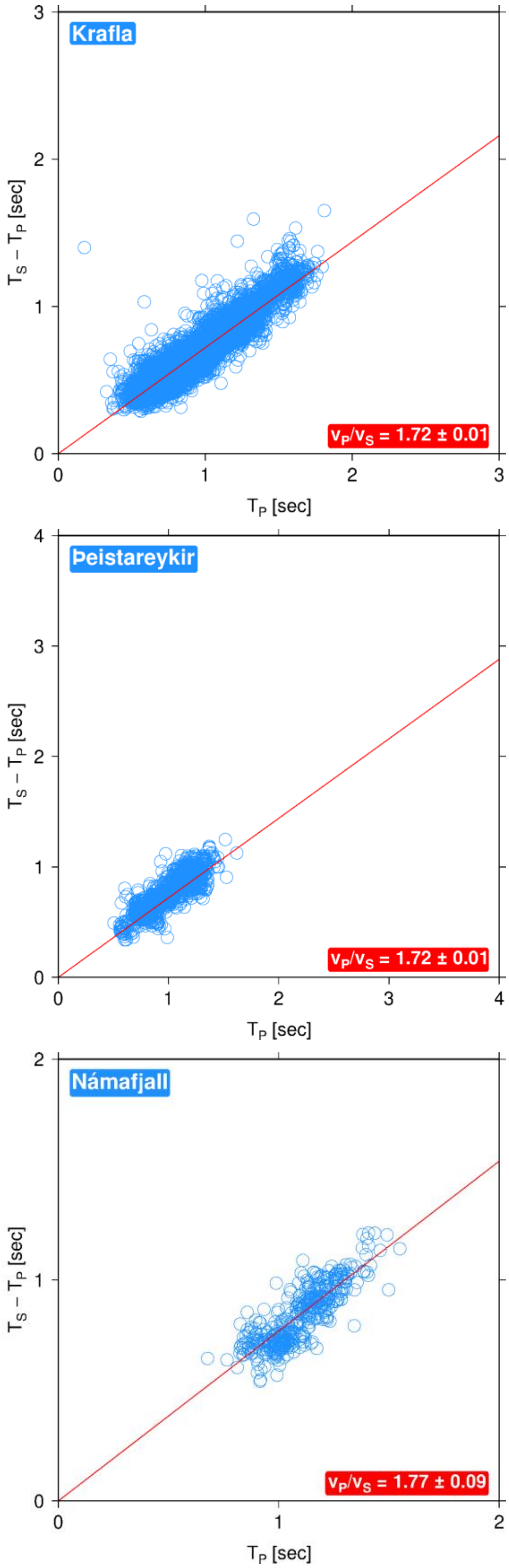

Figure C1. *Calculated Vp/Vs ratio for the Krafla, Þeistareykir and Námafjall geothermal areas during last year's study period (Oct. 2021 – Oct. 2022), from top to bottom, respectively.*